Reliability of Steam Turbine Rotors

EPRI

Keywords:
Rotor Lifetime
Boresonic Exam
Rotor Metallography
CrMoV Forgings
Retired Rotors
STRAP

EPRI NP-923-SY
Project 502
Summary Report
October 1978

Prepared by
Southwest Research Institute
San Antonio, Texas

ELECTRIC POWER RESEARCH INSTITUTE

Reliability of Steam Turbine Rotors

NP-923-SY
Research Project 502

Summary Report, October 1978

Prepared by

SOUTHWEST RESEARCH INSTITUTE
P.O. Drawer 28510
San Antonio, Texas 78284

Author
C. H. Wells

Prepared for

Electric Power Research Institute
3412 Hillview Avenue
Palo Alto, California 94304

EPRI Project Manager
Floyd E. Gelhaus
Nuclear Power Division

EPRI PERSPECTIVE

PROJECT DESCRIPTION

Turbine rotors are highly reliable components, with major failures occurring only once in several thousand turbine-years of operation. However, the consequential costs of even such infrequent failures are significant to the whole industry and are much larger than the direct costs of replacing a failed rotor. Following an intensive review of the Gallatin Unit-2 rotor burst and several earlier events, it was concluded that the phenomena involved were not necessarily unique and could be of generic concern to the utility industry. This conclusion led to project RP502, on the Reliability of Steam Turbine Rotors. This project is one of ten research efforts currently funded by EPRI related directly to various aspects of steam turbine performance. There are, in addition, nearly 30 other active projects whose results are to some degree related to the reliability of steam turbines.

PROJECT OBJECTIVE

The primary goal of this project is to develop a rotor lifetime prediction system to permit utilities to perform or confirm the analyses on which run-or-retire decisions are based. These analyses are best performed using actual operating histories and inspection data. However, the code system also can be utilized, in a parameter survey mode, to determine the sensitivity of the run/retire decisions to the completeness of the stress and fracture analysis models and to the uncertainties in the data on flaws, duty cycles, and properties. Inasmuch as inspection data are essential for valid analyses, another project objective has been to evaluate the state of the art of the nondestructive inspection systems and processes used in rotor bore examinations.

CONCLUSIONS AND RECOMMENDATIONS

The status of the project at this interim point is as follows. A Steam Turbine Rotor Analysis Program (STRAP), consisting of a computer code system, is completed, and the code is available from the EPRI Code Center. Although the fracture mechanics routine represents the state of the art, the data base does not adequately represent the linkup within clustered defects by crack growth across the ligaments,

especially under the combined effects of creep and low-cycle fatigue. The model for the change in material toughness due to aging embrittlement is also subject to improvement, because of the limited data so far available. Both effects are key aspects of the lifetime analysis. Two contractors (Commercial Machine Works and Westinghouse) have used the data obtained in evaluating current NDE systems in this project to improve their procedures. An important further step will be to verify the inspection techniques against flaws near the bore surface, and for radially-oriented fatigue cracks of various sizes. Improved discrimination in flaw sizing is an essential requirement for a definitive lifetime prediction system. In addition to the Gallatin rotor, two retired rotors were used for testing inspection systems and methods and for providing specimens for material properties measurements. Both rotors were taken out of service by the utilities who provided them on the basis of recommendations by the turbine manufacturers. On destructive examination, both were found to have only small, and relatively widely spaced, flaws. For one rotor, the calculations strongly suggest that the flaws are benign. The other rotor was found to exhibit significant temper embrittlement. This condition decreases the critical flaw size by a factor of about 4. Both rotors were indicated to be Class C. The existence of embrittlement in only one of the project rotors indicates a wide variation in the probability of embrittlement within the range of the Class C designation. These results highlight the ambiguities still present in both present NDE data and generic properties data that are used as the basis for run/retire decisions. Extension of the NDE work to additional rotors with a larger population of flaws including significant, non-benign flaws is needed to provide more generally applicable correlations. Advanced inspection techniques with better capability for flaw imaging and sizing are under development for other applications and are scheduled to be adapted for use on turbines.

The research effort to date has provided an improved interim tool for guiding run/retire decisions. It also provides a basis for future work aimed at producing more rigorous base for such decisions with fewer areas of ambiguity.

FUTURE WORK PLANNED AS A RESULT OF RP502

Continuing project effort is scheduled with the cooperation of the turbine facility of American Electric Power Service Corporation (AEP). AEP is providing the project with extensive facilities for rotor inspection and with a selection of retired rotors. A related supporting effort sponsored by AEP is contracted with Southwest Research Institute for development of an improved boresonic inspection system (TREES). The output from the TREES minicomputer will be used directly as input

to the STRAP calculations. Battelle Columbus Laboratories (BCL) will continue to focus on improved bore inspection system hardware and techniques. BCL will also adapt imaging methods and advanced signal processing techniques that have been developed on other NDE projects to the steam turbine rotor inspection process.

Floyd E. Gelhaus, Program Manager
Fault Analysis and Modeling Program
Nuclear Power Division

Blank Page

ABSTRACT

An automated Steam Turbine Rotor Analysis Program (STRAP) has been developed to facilitate the prediction of rotor lifetime given the duty cycle of the turbine and the results of ultrasonic examination from the rotor bore. STRAP consists in part of a preprocessor code that generates the boundary conditions and finite-element mesh for transient and steady-state temperature and stress analyses employing the ANSYS general-purpose structural analysis code. A postprocessor contains fracture toughness, stress-rupture, yield strength and fatigue crack growth rate data for air-melted 1 Cr-Mo-V forgings, on the basis of which the local stress and temperature values are screened to determine the critical crack size, the initial crack size that could grow to critical size within a specified number of hours or cycles and the minimum area fraction of defects which could link up to result in a significant crack. A boresonic data reduction code allows rapid sorting of indicated flaw sizes and locations to find the regions of greatest defect density.

At this stage of development, STRAP contains several deficiencies, which are the targets of the continuing RP502 effort. There are currently no means to assess the probability of temper embrittlement of an individual rotor short of determining the fracture appearance transition temperature, which has been found to be highly variable. No suitable crack growth algorithm has been developed for temperatures in the creep range, and an unequivocal interpretation of the TVA Gallatin rotor burst event in terms of measured mechanical properties is still being sought. Finally, the statistical correlation between ultrasonically-indicated defects and metallographically-determined sizes and spacings is inadequate, mainly because destructive sectioning of two retired rotors failed to reveal any flaws of structural significance.

Blank Page

ACKNOWLEDGMENTS

The RP502 project results represent the contractual combined efforts of Westinghouse Electric Co., Battelle Columbus Laboratories and Southwest Research Institute.

Mechanical property testing was conducted by E. T. Wessel and G. A. Clarke, Westinghouse Research and Development Center. Nondestructive rotor examination and system evaluation was directed by M. J. Golis and assisted by S. D. Brown and J. R. Fox, all of Battelle Columbus Laboratories. Sectioning of rotors and metallographic characterization of flaws were carried out by J. W. Cunningham, Westinghouse Research and Development Center. T. S. Cook and H. G. Pennick, Southwest Research Institute, developed the lifetime prediction analysis codes. The technical assistance of L. D. Kramer and R. R. Leyendecker, of Westinghouse Steam Turbine Division, is gratefully acknowledged.

Blank Page

CONTENTS

Blank Page

ILLUSTRATIONS

Blank Page

TABLES

SUMMARY

The material contained in this report is itself a summary of the results from the four task efforts:

Task	Description
1	Lifetime Prediction Analysis System;
2	Nondestructive Evaluation;
3	Destructive Tests; and
4	Properties Measurement

Separate Final Reports are available for each of these tasks, and the Steam Turbine Rotor Analysis Program (STRAP) is documented in a three-part manual. A copy of the STRAP code package along with the associated documentation is available from the EPRI Code Center.

The primary goal of this project is to develop a computerized rotor lifetime prediction system to assist utilities in performing run/retire analyses. These analyses can be completed by using actual steam turbine operational and inspection data or can be done on a parametric basis to further understand the sensitivity of the run/retire conclusion to key mechanistic assumptions and model approximations. A second major purpose of this research has been to evaluate the state-of-the-art of the non-destructive inspection systems and processes which are used in commercial rotor bore examinations.

The following are the salient RP502 research results to date, which are summarized within this document and further detailed in the appropriate task report.

- The limited comparison of the Steam Turbine Rotor Analysis Program (STRAP) stress-temperature results with independently calculated similar results has revealed no major disparities.
- The fracture mechanics code within the STRAP needs to be improved by adding a model for creep crack growth accompanied by intermittent stress-temperature cycling.

- The evaluation of two commercial non-destructive inspection systems indicates that the current state of the NDE can be improved through specific equipment improvements and procedural standardization.

- The NDE results emphasize the need to separate the inspection step of flaw detection from that of subsequent characterization.

- The destructive examinations showed that the variations in flaw reflectivity between different flaw types can so markedly change the reflected signal amplitude that using amplitude alone can result in a drastic error in sizing of the flaw.

- None of the destructive examinations revealed any crack interlinking of the imperfections.

- With the exception of two tests, none of the specimens from the failed Gallatin rotor exhibited the origin fracture mode (intergranular) under laboratory evaluation. The life reduction in those specimens with intergranular failure is not of sufficient magnitude to account for the Gallatin rotor failure.

- Of the two Class C rotors examined in the project, only one showed the presence of temper embrittlement, as reflected by a 300°F increase in the Fracture Appearance Transition Temperature (FATT). These data indicate the possibility of a marked variation in the level of embrittlement within the population of rotors designated to be Class C.

These project results to date have been utilized as motivation for improvements in existing rotor examination and lifetime evaluation procedures, and have produced the definitive set of concerns upon which the continuing research is focused.

Section 1

INTRODUCTION

This report summarizes the results of EPRI research project RP502, "Reliability of Steam Turbine Rotors," from January 1976 through March 1978. The project is continuing through 1980 towards the completion of a computerized lifetime prediction system that will allow a utility operator to assess the probability of rotor fracture from near-bore flaws as a function of continued service.

The goal of the project is a probabilistic lifetime prediction system that will incorporate the statistical distributions of stress, forging properties and flaw severity in calculating the time required for crack growth to unstable size. For several reasons these distributions are as yet unknown, and thus the analysis of lifetime is at present deterministic.

The origin of the RP502 project was the bursting fracture in June 1974 of the TVA Gallatin Plant Unit No. 2 IP rotor (1,2) from subsurface inclusions. The quantitative explanation of this rotor burst has provided a strong influence in selecting the failure modes included in the lifetime prediction system; however, the lifetime prediction system is intended to address all potential mechanisms of fracture under tangential stress in HP, IP, and LP rotors. Because of concern for the high defect concentration and fracture appearance transition temperature (FATT) of the air-melt 1 Cr-Mo-V Class C rotor forgings of 1950 vintage, project research has concentrated on evaluating the properties and ultrasonic response of this grade of material.

The current status of the RP502 project is summarized in Figure 1-1. The Steam Turbine Rotor Analysis Program (STRAP) consists of a geometry and heat transfer preprocessor (PPMESH) and a fracture analysis postprocessor (FRAC) written for a general-purpose structural analysis computer code (ANSYS). The preprocessor accepts the principal dimensions of the rotor, blade weights, interstage seal configuration, and end conditions such as the steam or water shaft seals. The user must specify the history of rotor speed, steam inlet and outlet temperature and pressure, and shaft seal fluid temperature. The preprocessor then generates

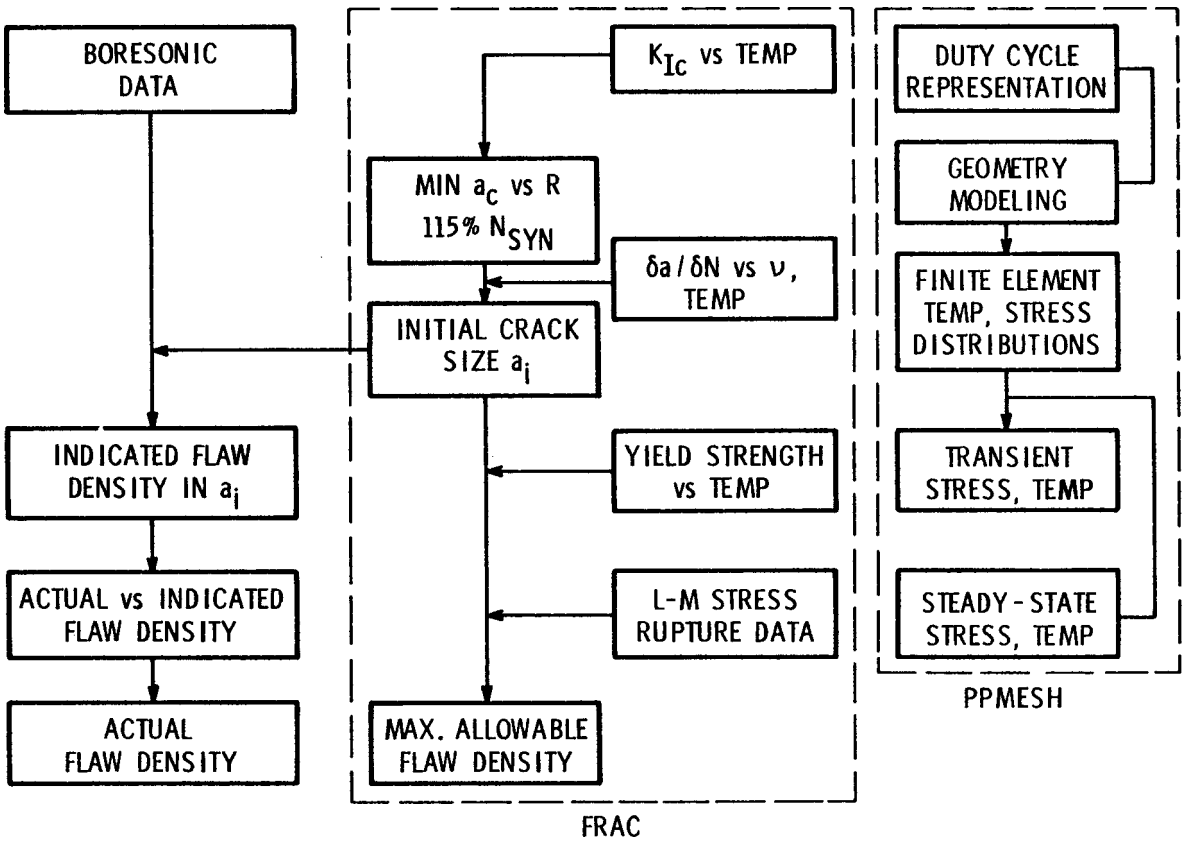

Figure 1-1. Steam Turbine Rotor Analysis Program (STRAP)

the finite element model of the rotor, calculates blade loads, steam leakage flow and heat transfer coefficients, and manages the transient temperature distribution analysis by the ANSYS code. Then the combined thermal and centrifugal stress distribution is calculated at a sufficient number of time steps to determine the peak transient and steady-state values of stress at the centroid of each element. These values are stored for fracture analysis.

Since the STRAP system represents a compromise between generality and the cost and complexity of use, it will not handle some rotor configurations currently in service. For example, it does not allow the prescription of a variable thickness

disk or large diameter changes between sections of integral rotors, nor does it provide an accurate analysis of local stresses near the periphery of the rotor. It should be emphasized that these constraints arise due to the automation of the mesh generation. The preprocessor can be modified to accept virtually any geometry, but at the cost of increased complexity of input and operation.

The FRAC code provides a number of computations for possible failure modes, brittle fracture, ductile fracture, low-cycle fatigue crack growth, and stress rupture. It does not contain provision for stress corrosion cracking or for creep crack growth, or for cracking in bending or torsional fatigue. Methods are contained for predicting the growth and criticality of isolated flaws of various shapes as well as three-dimensional distributions of flaws. The statistical representation of fracture properties for 1 Cr-Mo-V forgings requires the resolution of two major problems. One involves the susceptibility to temper embrittlement at service temperature, which has been found in one rotor to have resulted in an increase in FATT of 300°F. It is not known whether the probability of such embrittlement can be predicted from the available history of a forging or whether metallographic or fracture tests will have to be performed on coupons from the rotor. The other problem is the variability of creep crack growth rate, which requires the acquisition of a data base and the development of a crack growth algorithm. Both problems are being addressed as part of the continuation of RP502.

The greatest source of uncertainty in lifetime prediction of rotors at present must be attributed to the boresonic examination procedure. The STRAP is intended ultimately to accept the data from boresonic analysis and statistically assess the severity of the flaws in terms of the probability of crack growth rate to critical size. The statistical correlation between boresonic indications and equivalent crack size and spacing has not been established at this time, primarily becuase the rotors selected for destructive evaluation of indications were found to contain low densities of very small flaws. The boresonic identification of these small flaws indicated poor reproducibility of density and essentially no correlation between signal amplitude and flaw size; however, these sizes and densities are well below the range of practical significance. In addition, the capability of boresonic examination to size radial-axial fatigue cracks was not determined. Notwithstanding these results, sufficient transducer, mechanical drive, and electronics system characterization was completed to allow optimization of conventional ultrasonic procedures for rotor evaluation, and such an optimized system will be constructed under the continuation of the project.

The current procedure for determining rotor integrity from boresonic results, as shown in Figure 1-2 is to reduce the indications to an area fraction on a radial-axial plane and to assume conservatively that circumscribed regions of high area fraction represent cracks. What constitutes a "high" area fraction, of course, is largely subjective, given the lack of confidence in amplitude indications, and should be related to the ratio of the local stress to the yield stress or stress to produce rupture. This judgement must be supplied by the operator since the data reduction program for boresonic results is currently independent of the lifetime prediction analysis system. For example, the interaction distance between distributed flaws is estimated by linear elastic fracture mechanics and is assumed independent of stress, whereas the extent of out-of-plane (tangential) linkup has been shown to increase significantly with stress. Incorporation of this variable interaction distance into an advanced version of the FRAC postprocessor is expected to require nonlinear fracture mechanics analysis, as is the effect of ligament width on near-bore crack growth behavior.

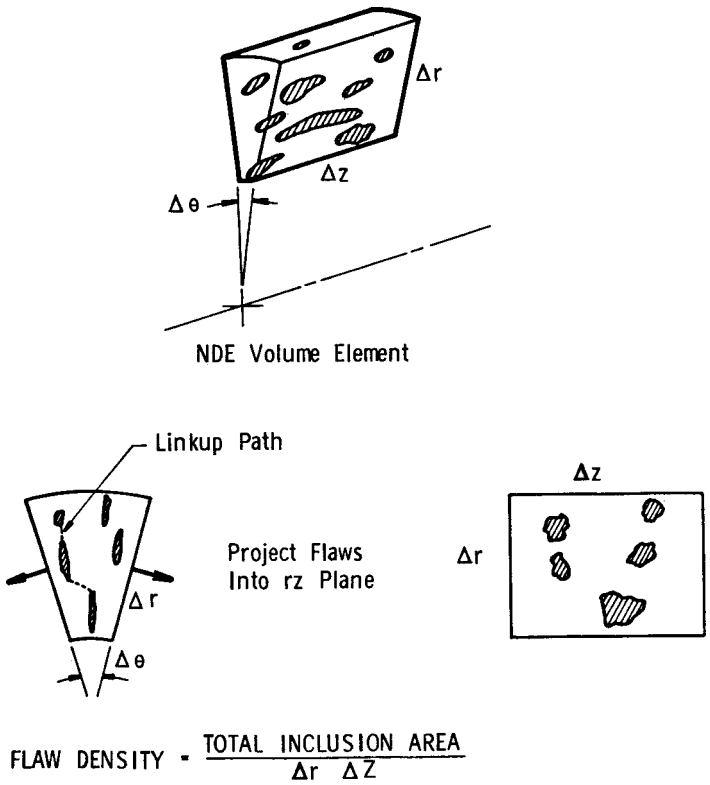

Figure 1-2. Boresonic Data Reduction

Accurate prediction of linkup between clustered defects requires much higher resolution of flaw size than is available with commercial boresonic systems. An advanced system, incorporating focused and collimated transducers and on-line data reduction compatible with the STRAP, is slated for development during the continuation of the project.

Mechanical property characterization of air melt 1 Cr-Mo-V forgings has included fracture toughness data and its correlation with FATT, and fatigue crack propagation data at elevated temperatures with hold times up to 24 hrs per cycle. Stress rupture data was compiled from a number of sources, including the Metal Properties Council creep-fatigue interspersion testing project (3). Despite intensive effort to duplicate the TVA Gallatin rotor burst mechanism, the RP502 data base is apparently non-conservative in that it does not predict the lifetime of the Gallatin rotor with the best estimates of operating conditions. The conclusion of this effort is that while the material in the initiation region of the rotor may have been marginally deficient with respect to intergranular crack growth resistance, data for creep crack growth accompanied by intermittent cycling is needed in order to predict the fracture life. This data will be acquired in the continuation of contract effort.

The following sections detail the progress made in various aspects of the project.

REFERENCES

1. L. D. Kramer and D. Randolph, "Analysis of TVA Gallatin No. 2 Rotor Burst. Part I - Metallurgical Consideration," 1976 ASME-MPC Symposium on Creep-Fatigue Interaction, R. M. Curran, Ed., American Society of Mechanical Engineers, G00112, 1976, p. 1.

2. D. A. Weisz, "Analysis of TVA Gallatin No. 2 Rotor Burst. Part II - Mechanical Analysis," Ibid., p. 25.

3. R. M. Curran and B. M. Wundt, "Continuation of a Study of Low-Cycle Fatigue and Creep Interaction in Steels at Elevated Temperatures," Ibid., p. 203.

Section 2

STEAM TURBINE ROTOR ANALYSIS PROGRAM (STRAP)

The STRAP system consists of the geometry and heat transfer preprocessor (PPMESH), the fracture analysis postprocessor (FRAC), and the boresonic data reduction program, shown in Figure 1-1. Programmer's guides and user's manuals for these codes have been prepared (1 - 4) and describe in depth the assumptions, calculations, logic flow, and data base involved in the assessment of rotor reliability. Thus only a summary of these codes will be presented here.

FRAC and PPMESH were written for the proprietary ANSYS (5) general purpose finite element structural analysis program after a comparison of the cost and technical capabilities of the most promising codes (6). STRAP can be used on any large computer system such as the CDC 6600 or 7600 and IBM 360/155. It is, however, not cost-effective to reduce the boresonic data on a large main-frame computer.

The objective of these codes has been to provide as complete, yet inexpensive analysis as possible for a utility operator while maintaining sufficient flexibility to model a number of rotor configurations and calculate transient thermal stress with reasonable accuracy.

TEMPERATURE ANALYSIS

Transient temperature calculations, such as illustrated in Figure 2-1, often show temperature differences of as much as one hundred degrees between bulk steam and rotor surface; thus an estimate of heat transfer coefficients is necessary. The heat transfer coefficients depend upon steam leakage flows and seal configurations, rotor surface speed, and steam properties. The expressions for convective heat transfer coefficients are given in the PPMESH Programer's Guide (1). In addition, an equivalent resistance for heat conduction from the blading to the disk rims was developed. The transient thermal analysis thus requires the operator to specify seal geometry and steam inlet and outlet temperature and pressure as functions of time. The physical properties of steam and the rotor steel are built into PPMESH. A single seal geometry giving the maximum leakage flow (min-

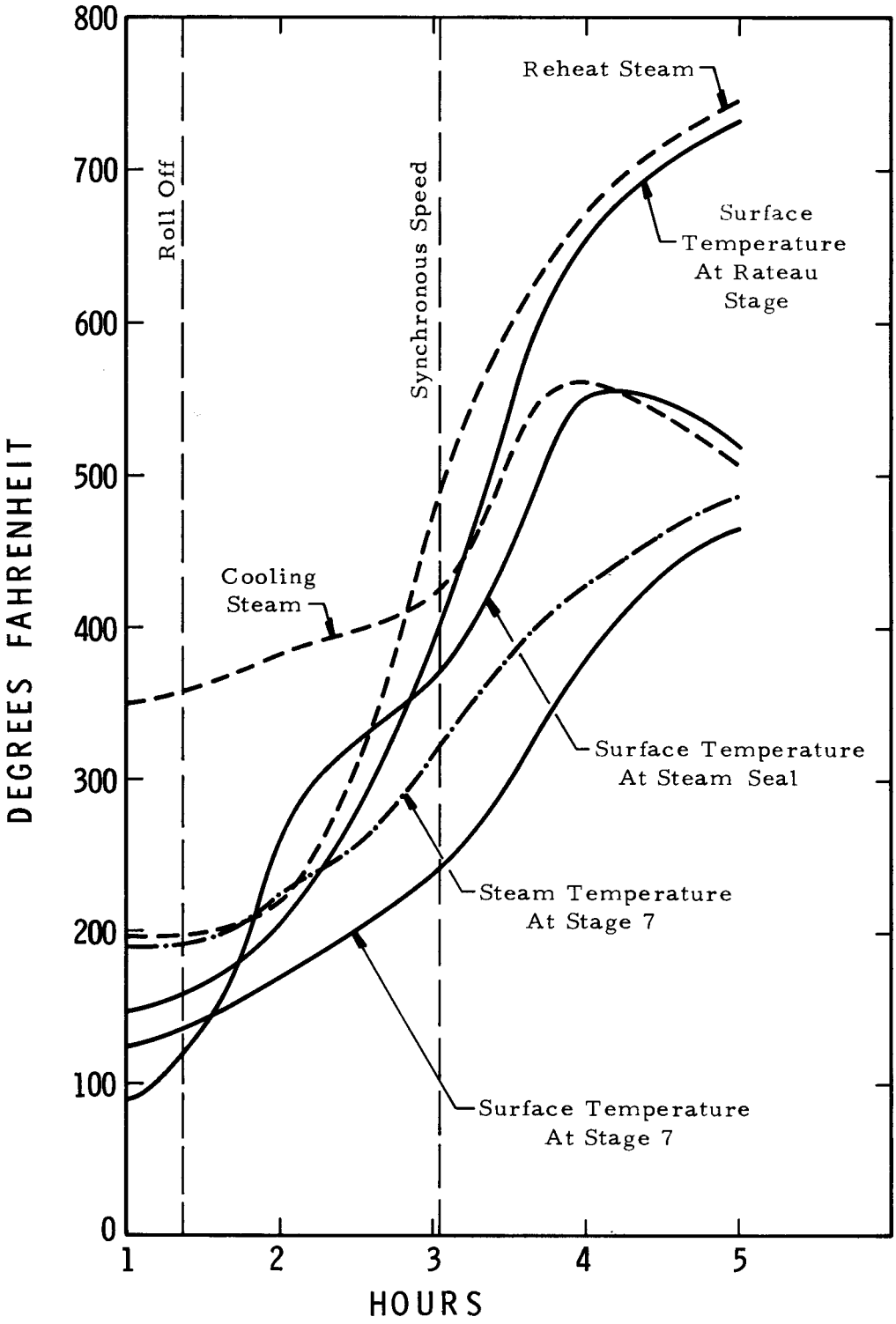

Figure 2-1. Gallatin No. 2 IP Transient Steam and Surface Temperatures

imum number of teeth, maximum clearance) must be specified; the transient rotor temperature is relatively insensitive to seal geometry. Leakage flows are calculated from Martin's equations (7), and the heat transfer coefficients on the rotor surface from the correlation given by Kapinos and Gura (8). Other rotor sections are modeled as rotating cylinders and disks.

While the description of the boundary conditions is considered reasonably complete, it may not include certain important factors such as secondary flows and the degree of turbulence, which may differ from that developed in the experiments upon which the correlations used for disks and cylinders were based. The transient temperatures calculated by the PPMESH/ANSYS code have not been experimentally verified, but plans have been made to conduct such verification tests under a separate EPRI program.

The duty cycle representation usually consists of three parts, prewarming, roll-off to paralleling, and from no load to full load. The preprocessor does not contain the steam expansion lines from the Mollier diagram, but distributes the pressure and temperature drops across each reaction stage according to experimental extraction point data given the time variation of inlet and outlet steam conditions. The experimental data was obtained from General Electric and Westinghouse turbines, and is adjusted for different percentage pressure drops across the stator and rotor blading. Often the steam conditions prior to attaining synchronous speed are not available; in such cases it is usually easy to assume a conservative startup history. STRAP will accept any arbitrary history of steam conditions and rotor speed. Figure 2-2 shows an example of the transient temperature distribution calculated for the Gallatin No. 2 IP rotor after 0.85 hours of loading. The steady state distribution is given in Figure 2-3.

STRESS ANALYSIS

The stress analysis requires estimates of blade weight for each stage. Values of Young's modulus versus temperature are included in PPMESH, along with the material thermal properties. Centroidal values of tangential stress are calculated and stored with the corresponding temperatures at each time step. The code contains interpolation and extrapolation algorithms to determine the stress at any (r,z) location. The stress analysis does not include inelastic material response (although ANSYS has the capability of performing elastic-plastic and creep calculations). Since the automatic mesh generation was designed to provide

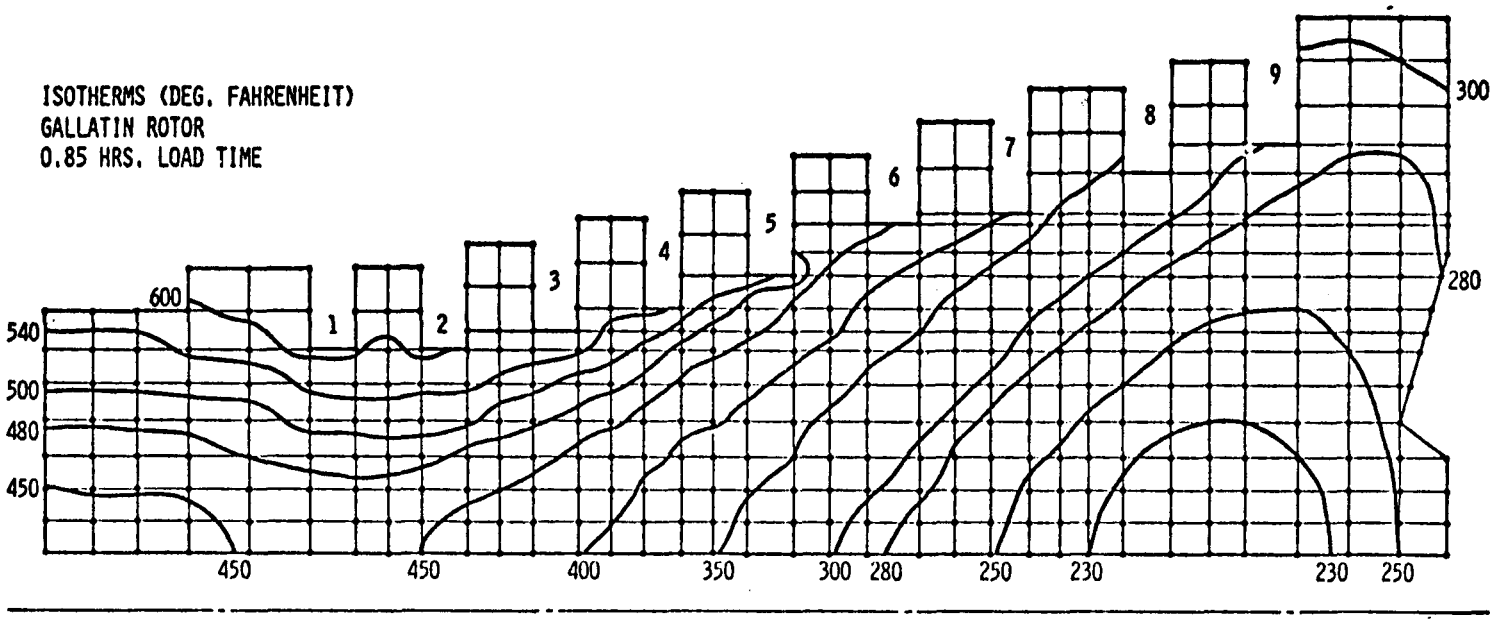

Figure 2-2. Gallatin No. 2 IP Transient Temperature Distribution

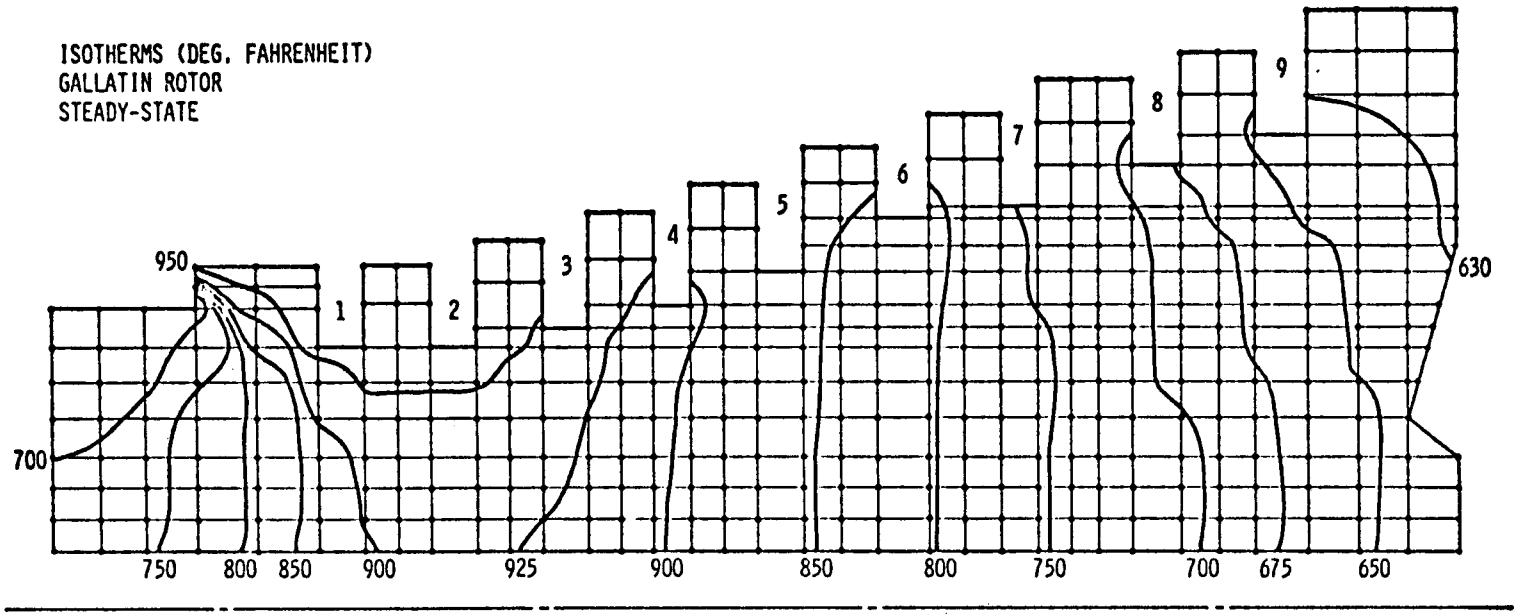

Figure 2-3. Gallatin No. 2 IP Steady-State Temperature Distribution

accurate stress distributions only out to around 4 in. radial distance from the bore surface, the stresses near the periphery of the rotor are not sufficiently accurate for calculations of diaphragm groove or disk rim cracking. Figure 2-4 shows the distribution of tangential stress in the Gallatin IP rotor at the time (during startup) of maximum tangential stress; comparison of these predictions with the results of independent calculations by Westinghouse (9) shows good agreement.

ROTOR ANALYSES

In addition to the Gallatin rotor, complete temperature and stress calculations were conducted on two rotors selected for boresonic and destructive examination (Electric Energy Inc. Joppa No. 3 IP, Duke Power Co. Buck No. 6 IP-LP) and a low-pressure rotor which had been independently analyzed elsewhere (Pennsylvania Electric Co. Seward No. 5). Also, the STRAP system was used to analyze an integral IP-LP rotor (American Electric Power Sporn Series). Complete details of these analyses are contained in the Task I Final Report (10) and are merely summarized here. Table 2-1 lists the most significant results--namely, the time, temperature, and magnitude of the maximum tangential stress and the temperature and magnitude of the steady-state stress at the same location. Note that the maximum steady state stress does not always occur at the same location as the maximum transient stress: of the five rotors analyzed, two had maximum values at different locations. Time to maximum stress is measured from the commencement of loading during a cold start. The maximum stress is calculated for synchronous speed, i.e., no overspeed. Differences in steady-state stress values may be attributed to design differneces, while differences in peak transient (thermal) values reflect the loading rate of the turbo-generator. The maximum tangential stress is not precisely equal to the sum of the peak transient and steady-state stresses, since some thermal stress is present during steady-state operation.

The transient and steady-state temperature and stress values are filed for search by the FRAC postprocessor and usually provided in hard copy as well as computer graphics, e.g., Figures 2-5 and 2-6, which show isotherms and isostress lines for the Seward LP rotor, respectively.

FRACTURE ANALYSIS

Guided in part by the Gallatin No. 2 IP fracture, the initial assumption was made that subcritical crack growth from multiple defects could be described by linear elastic fracture mechanics using elevated-temperature fatigue crack propagation

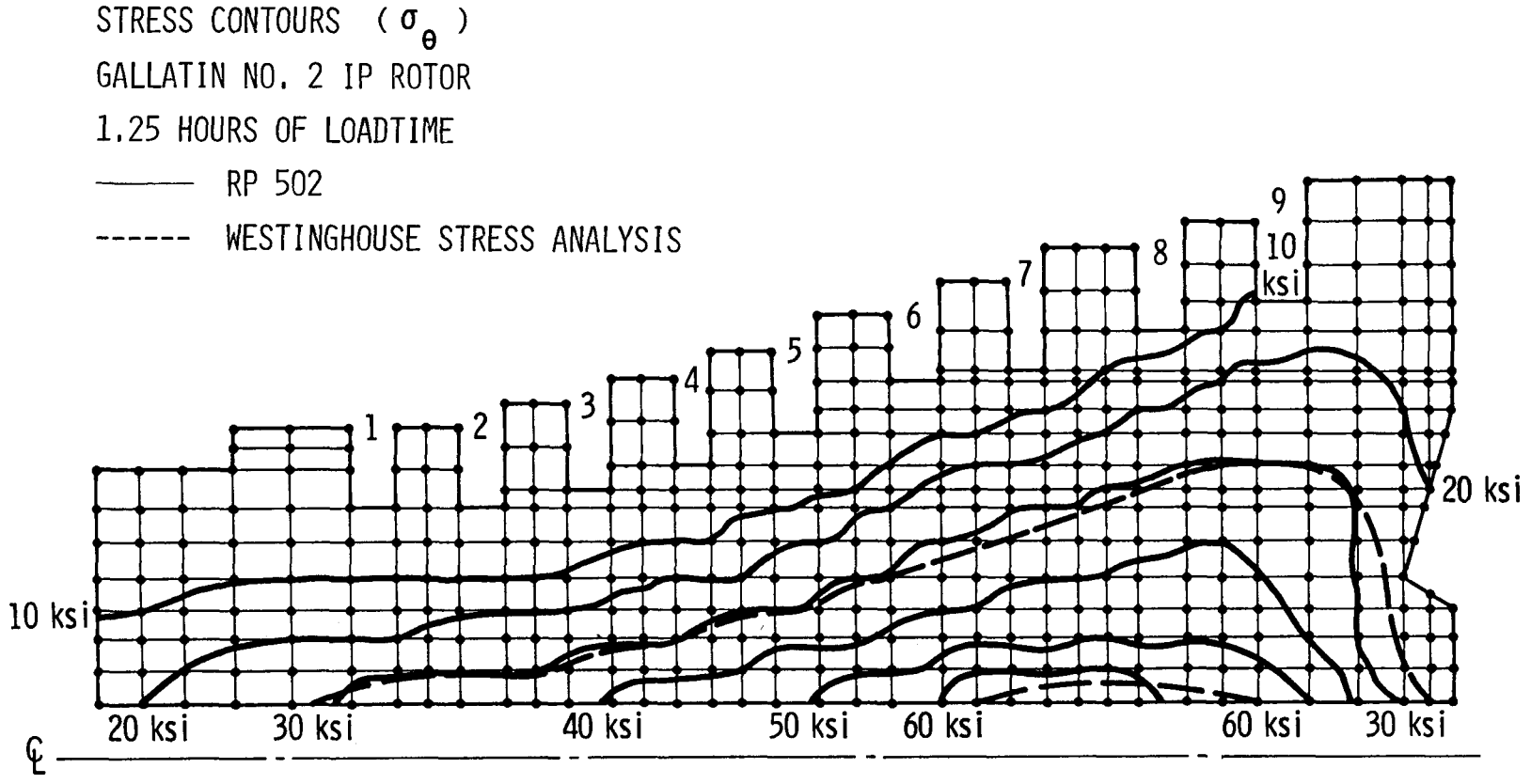

Figure 2-4. Tangential Stress Contours At Time Of Maximum Stress

Table 2-1

MAXIMUM TANGENTIAL ROTOR STRESSES AT SYNCHRONOUS SPEED

Rotor	Transient[1]			Steady State[1]	
	σ_θ, ksi	T, °F	τ, hrs[2]	σ_θ, ksi	T, °F
Gallatin No. 2 IP					
	74.0	272	1.25	47.2	727
Joppa No. 3 IP					
	37.0	308	1.50	31.0	450
Seward No. 5 LP					
	39.4	163	1.00	21.5[3]	302
Buck No. 6 IP-LP					
	56.0	344	0.60	13.9[3]	884
Sporn Series IP-LP					
(Cold Start)	23.2	421	2.80	17.4	526
(Hot Start)	27.4	615	1.00		

[1]Stresses are computed at element centroids and extrapolated to the bore.

[2]Time after start of loading.

[3]Maximum steady state stress did not occur at location of maximum transient stress.

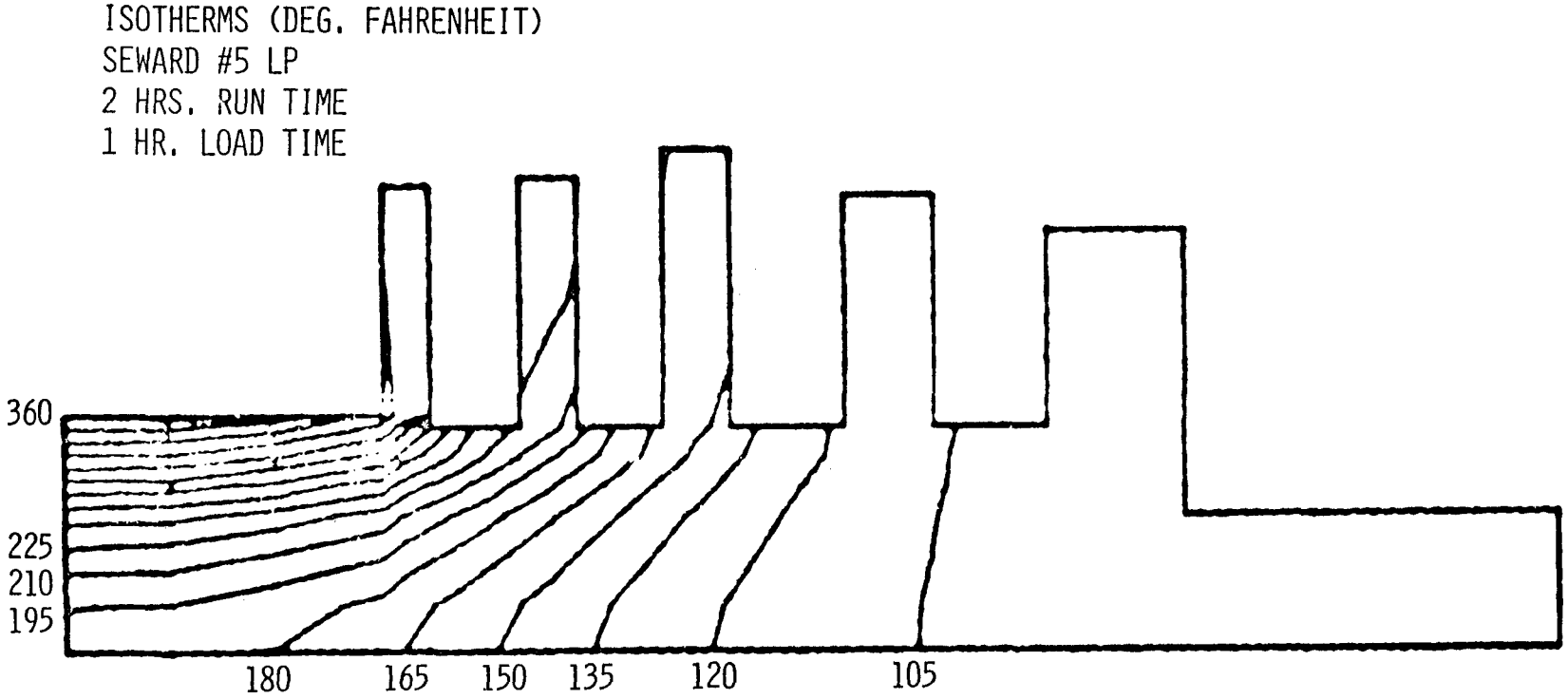

Figure 2-5. Computer-Drawn Isotherms For Seward No. 5

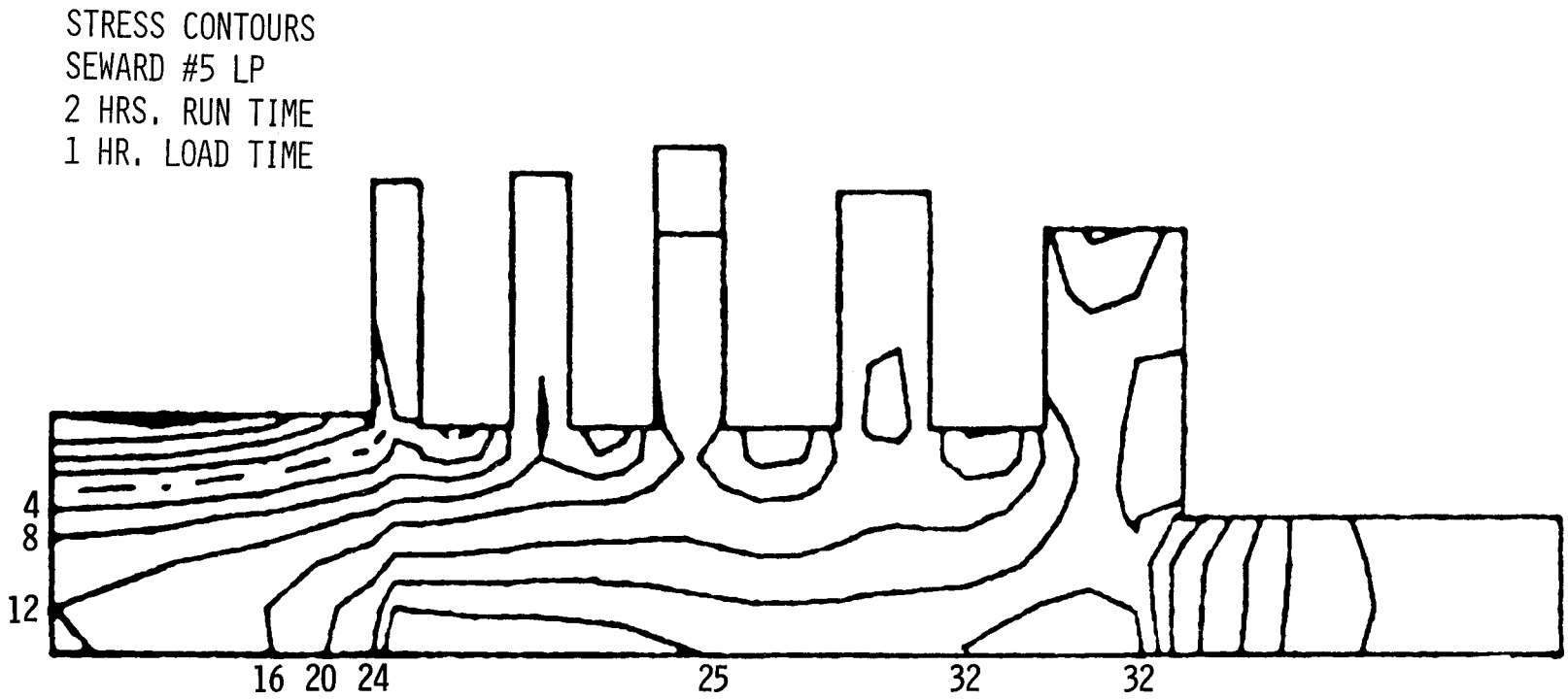

Figure 2-6. Computer-Drawn Isostress Lines for Seward No. 5

data. Calculations of crack growth from small inclusions via conventional fracture mechanics showed that the amount of growth predicted for 1000 cold starts (a conservatively large number, since most rotors have been subjected to around 200-300 starts in 20 years) is negligible. For example, if the maximum stress and temperature are assumed to coincide at the initiation site of the Gallatin rotor, the crack growth from a 0.188-in. inclusion in 1000 cycles using the maximum growth rate observed is only 0.009 inch. The low-cycle fatigue crack growth in a peaking cycle turbine may be more significant, since a daily startup will lead to the accumulation of around 10,000 cycles in a lifetime of 30 years. In this case, however, most starts are hot, and the stress is more nearly equal to the steady-state value; thus the fatigue damage would be expected to be more significant in low-pressure rotors and in the cold end of intermediate-pressure rotors. In the hypothetical case of a Gallatin IP rotor in a power peaking application, the crack growth from the inclusion cited above would be only 0.026 inch.

Large cracks and crack-like boresonic indications have been reported in several rotor designs other than Gallatin No. 2, and since the objective of the RP502 analysis system is to assist in evaluating the integrity of rotors approaching retirement, several mechanisms of fracture have been included in the post processor. Regardless of mechanism, the critical crack size for catastrophic fracture is of concern since it serves as the terminal point of subcritical crack growth. The critical crack size is a function of geometry (e.g. aspect ratio of the crack, proximity of the bore surface or of neighboring cracks), local stress and temperature. Temperature governs the local fracture toughness, as discussed in Section 4.

Critical Crack Size Calculation

The critical value of stress intensity factor, K_{IC}, or of path-independent J-integral (11), appears to correlate with the unstable propagation of a crack and has been built into FRAC as the first step in fracture analysis. Because of the possibility of overspeed on startup, and in view of the requirement to test overspeed trips, a nominal overspeed of 15 percent of synchronous is assumed in FRAC; however, any other value can be specified by the STRAP user. The values of critical crack size are calculated for user-selected flaw coordinates, and flaw aspect ratios of 1, 3, and ∞ can be selected if the results of a boresonic examination are available. If inspection data is not available, FRAC determines the axial location of the minimum critical flaw size and its variation with distance from the bore surface, thereby specifying the areas over which the boresonic

data reduction must be carried out. FRAC is capable of interaction with an automated boresonic system when warranted, but at the present time the data input and output are handled manually.

The location of the minimum critical crack size usually coincides with that of the maximum tangential stress; however, it is possible that lower-stressed regions might exhibit a smaller value because of lower fracture toughness. Lower toughness may result from the local stress peaking at a lower temperature or from temper embrittlement of those portions of the rotor subjected to high service temperature.

The FRAC code examines such areas to ascertain the minimum critical crack size. Table 2-2 shows the results determined for the rotors in Table 2-1, where the critical flaw has been assumed to occur at the bore surface.

A modification to the critical flaw size calculation is required to take into account the presence of temper embrittlement, or large, service-induced increases in FATT. Such an increase, on the order of 300°F, was recently found near the inlet end of the Buck No. 6 rotor, where the steady-state temperature was calculated to be around 900°F. No increases in FATT were determined for Gallatin No. 2 or for Joppa No. 3, which was similar to Buck No. 6 with respect to age, service exposure and composition. Both the Joppa and Buck rotors were reported to be Class C forgings. The factors governing the susceptibility to temper embrittlement, believed to be a high final austenitizing temperature with concomitantly coarse prior austenite grains, along with high levels of trace elements, have not yet been identified. Of particular concern is the probability of embrittlement within the range of the Class C designation. At this time it appears that, as a minimum, a separate fracture toughness data base must be generated for susceptible forgings such as Buck No. 6, and that this data base must represent the extent of embrittlement as a function of the local steady-state service temperature. In determining the critical crack size, the FRAC code must select the curve of fracture toughness versus instantaneous temperature corresponding to the steady-state temperature.

Table 2-2 illustrates the impact of the increased FATT on the critical crack radius. In the case of embrittlement, the critical crack location shifts to the inlet end of the rotor. The material has been assumed to have a K_{IC} value of 30 ksi $\sqrt{in.}$ below 600°F in this comparison.

Table 2-2

CRITICAL RADIUS OF SEMICIRCULAR BORE CRACK

	a_c, inches	
	Unembrittled	Embrittled*
Gallatin No. 2 IP	0.27	N/A
Joppa No. 3 IP	1.10	N/A
Seward No. 5 LP	0.77	N/A
Buck No. 6 IP-LP	0.68	0.18
Sporn Series IP-LP	3.37	0.82

*300°F increase in FATT

Another required modification is the inclusion of the effect of the bore surface on nearby imbedded flaws, wherein the lack of plane strain constraint amplifies the stress intensity factor. Currently FRAC includes an empirical correction factor for the near surface based upon the work of Brandt (12). Data acquisition and elastic-plastic analyses are underway in the continuing RP502 contract in order to correct these deficiencies.

Initial Crack Size Calculation

Having determined the critical crack size, FRAC next calculates the initial crack size that could grow to critical size within a user-specified number of duty cycles. Alternatively, the user may specify an initial crack size, based upon the boresonic results, and calculate the number of cycles required to reach critical size. The data base for these calculations is described in Section 4. The size thus calculated represents an isolated, crack-like flaw in a radial-axial plane that could grow to critical size in the specified duty cycles. This size is shown as a function of distance from the bore surface for the Gallatin No. 2 IP rotor in Figure 2-7. (The results given in Figure 2-7 reflect the original perception of the Gallatin failure as the result of fatigue link-up of neighboring inclusions; the plots shown were therefore made using the unit cell geometry of (6) to account for nearest-neighbor interaction. A semicircular, bore-connected crack was assumed in the comparison in Table 2-2. Since the two flaw

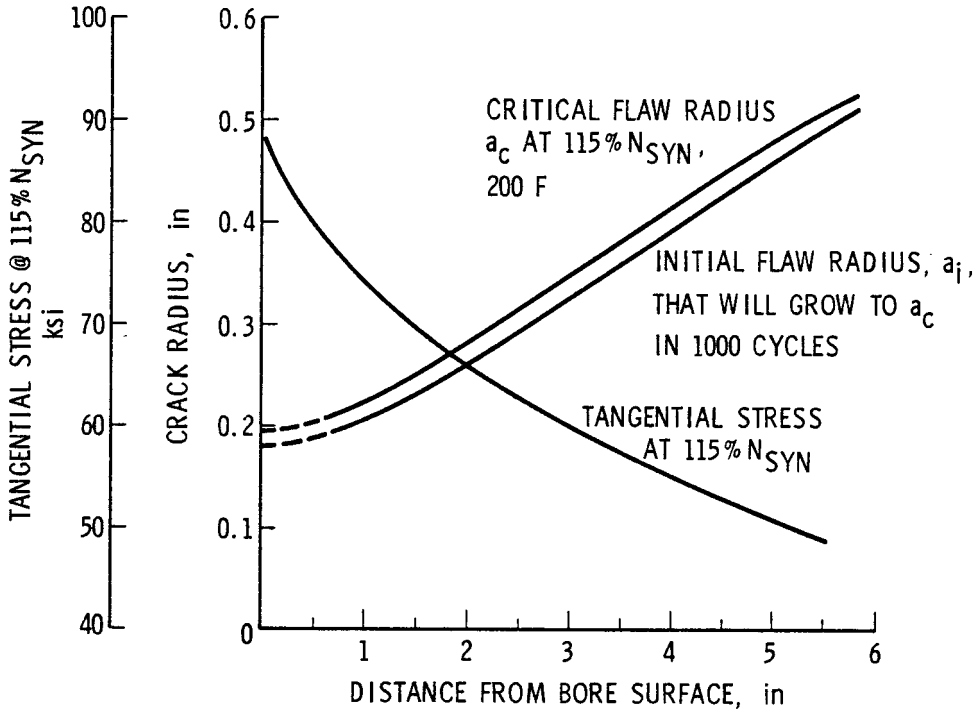

Figure 2-7. Variation Of Initial Crack Size With Radius For Gallatin No. 2 IP

geometries are different, the results of the two Gallatin computations are slightly different.) At temperatures above about 750°F, cracks can grow by a time-dependent creep rupture mechanism (13). While intensive evaluation of creep crack growth is underway in England, no data appears to have been generated in the United States, and none is currently available for inclusion in the RP502 system.

Cluster Analysis

While the detection and evaluation of isolated cracks is relatively straightforward, a general and complex problem in the steam turbine industry appears to be the assessment of distributed, three-dimensional arrays of defects commonly called clusters. Such a cluster or clusters of small manganese sulfide inclusions reportedly provided the initiation sites of the Gallatin fracture. Predicting the linkup between distributed flaws in a cluster requires several steps:

1. Determination of the interaction distance between neighboring flaws, especially that distance in the circumferential direction normal to the (radial-axial) plane of fracture over which flaws link up;

2. Calculation of an effective area fraction of flaws where the boresonic examination does not supply individual flaw sizes;

3. Calculation of progressive linkup by fracture mechanics where flaw sizes are known from boresonic data; and

4. Determination of the criteria for inelastic instability by ligament yielding and for ligament creep rupture.

The problems of boresonic examination of clusters and data reduction are discussed in Section 3. The interaction distance is currently determined by linear elastic fracture mechanics, which predicts that two cracks will interact to increase significantly the stress intensity factor in the ligament between them only when their separation is on the order of twice the diameter of the larger crack. As the net ligament stress (nominal stress divided by the uncracked area fraction) approaches the yield stress or, in fracture mechanics terminology, if the plastic zones of two adjacent crack tips reach a large fraction of the ligament width, the interaction distance increases markedly. The FRAC postprocessor does not currently incorporate this effect of nonlinear material behavior, which requires elastic-plastic analysis. Two other contributing factors are believed to be hydrostatic tensile stress, which concentrates shear strain between adjacent flaws (14) and cyclic deformation. However, FRAC does contain a conservative criterion for cluster linkup taken from the work of Melville (15), which states that when the net ligament stress equals the yield stress, the ligaments are assumed to fail, leading to an "unzipping" process at overspeed during a single cycle. This criterion is very conservative, since it is known that such clusters can resist many cycles of reversed plastic strain before linkup occurs (see Section 4). Although irrelevant to the actual failure mode of the Gallatin rotor, this criterion in STRAP would have dictated the retirement of the rotor. Similarly, the net ligament stress during steady-state operation is compared to the stress to produce rupture at the steady-state temperature within a specified time period. However, in the case of stress rupture, the criterion cannot at this point be judged to be conservative in view of the inability to predict the Gallatin rotor burst. The data and its interpretation are discussed in Section 4.

Regardless of the net ligament stress, it is obvious that fracture cannot ensue unless the extent of flaw linkup is at least equal to the area of the initial

crack size which can grow to the critical size in the specified operating time. Thus the user can compare the calculated area fractions and initial crack sizes with boresonic data to evaluate the severity of the cluster. It follows that one of the essential requirements for boresonic examination is the ability to discriminate between uncracked clusters and clustered flaws with crack extension tending to link them together.

REFERENCES

1. H. G. Pennick, T. S. Cook, and C. H. Wells, Programmer's Guide for the Analysis of Thermoelastic Stresses in Steam Turbine Spindles, Report on EPRI Project RP502, June 1977.

2. H. G. Pennick, T. S. Cook, and C. H. Wells, User's Manual for PPMESH Preprocessor and Mesh Generating Program, Report on EPRI Project RP502, June 1977.

3. H. G. Pennick, T. S. Cook, and C. H. Wells, Programmer's Guide for the Fracture Analysis of Steam Turbine Spindles, Report on EPRI Project RP502, April 1978.

4. H. G. Pennick, T. S. Cook, and C. H. Wells, User's Manual for FRAC Fracture Analysis Program, Report on EPRI Project RP502, April 1978.

5. J. A. Swanson, ANSYS - Engineering Analysis System User's Manual, Swanson Analysis System, Inc., Elizabeth, Penna., 1975.

6. C. H. Wells and T. S. Cook, First Semiannual Progress Report on EPRI Project RP502, July 1976.

7. H. M. Martin, "Steam Leakage in Dummies of the Ljungstrom Type", Engineering, 3 January 1919, p. 1.

8. V. M. Kapinos and L. A. Gura, "Investigation of Heat Transfer in Labyrinth Glands on Static Models", Teploenergetika, 17, 11, 1970, p. 38-41.

9. D. A. Weisz, "Analysis of TVA Gallatin No. 2 Rotor Burst. Part II - Mechanical Analysis", 1976 ASME-MPC Symposium on Creep-Fatigue Interaction, R. M. Curran, Ed., American Society of Mechanical Engineers, G00112, 1976, p. 25.

10. T. S. Cook, H. G. Pennick, and C. H. Wells, Task I Final Report on EPRI Project RP502, April 1978.

11. J. A. Begley and J. D. Landes, "The J Integral as a Fracture Criterion," Fracture Toughness, ASTM STP 514, 1972, p. 1.

12. D. E. Brandt, "The Development of a Turbine Wheel Design Criterion Based upon Fracture Mechanics," J. of Engineering for Power, Trans. ASME, 93, Oct. 1971, p. 411.

13. C. B. Harrison and G. N. Sandor, "High-Temperature Crack Growth in Low Cycle Fatigue," Engng. Frac. Mech., 3, 4, Dec. 1971, p. 403.

14. S. I. Oh and S. Kobayashi, "Deformation Mode of Void-Growth and Coalescence in the Process of Ductile Fracture," AFML-TR-75-95, July 1975.

15. P. H. Melville, "Fracture Assessment for Inclusion Clouds in Large Rotor Forgings," Central Electricity Generating Board Report RD/L/N47/76, May 1976.

Section 3

NONDESTRUCTIVE EVALUATION

The run-retire decision-making process requires that the initial quality of the rotor forgings as well as service-induced damage be quantitatively defined for evaluation according to the various fracture modes assumed by the FRAC postprocessor. Certain bulk property changes, such as creep cavitation and temper embrittlement, and initial microstructural variations cannot be evaluated nondestructively and must ultimately reflect the statistical influences of chemistry, ingot solidification and forging thermal-mechanical history. This aspect is discussed in Section 4.

Nondestructive evaluation involves the detection and characterization of macroscopic defects, such as nonmetallic inclusions and porosity, that constitute the origins of fracture, and of service-induced cracks. The RP502 project has concentrated on the evaluation of commercial methods of ultrasonic testing from the rotor bore hole out to distances of around four inches from the bore surface, with some characterization of near-bore magnetic methods. The performance of two commercial systems on two retired intermediate-pressure rotors (Joppa No. 3, Buck No. 6) was initially studied without any attempt to optimize the inspection procedure. Subsequently, limited reinspection was conducted with variations in the transducer and mechanical drive parameters to arrive at an optimized state-of-the-art procedure. Laboratory tests on artificially-flawed blocks augmented this evaluation. The details of this performance study have been published in Ref. (1), and only the most significant results will be repeated here.

The most critical link between nondestructive evaluation and lifetime prediction is the determination of the size and spacing of defects and the extent of crack propagation from them. Since the maximum tensile stress developed in the rotor is tangential, the corresponding crack growth is primarily in a radial-axial plane; consequently, the dominant flaws are those with the largest projected area in the (r,z) plane, and the most severe clusters are those with large area fractions on such a plane. In the case of clusters containing flaws which are not coplanar, it is necessary to account for out-of-plane linkup between flaws over some tangential distance, as will be discussed below (see also

Fig. 1-2). In making run-retire decisions, the utility operator does not have the advantage of the extensive correlation between forging quality and rotor reliability which has been acquired by the manufacturers, nor is it practical to duplicate independently such a statistical data base. The utility operator accordingly requires a higher degree of certainty in the sizing and location of flaws and in the ability to discriminate between flaws which have initiated cracks and those which have not.

Both isolated (r,z) cracks and high-density clusters containing cracks are of major concern from a reliability standpoint. The capability of detecting fatigue cracks has not yet been evaluated under the RP502 project, although the response from an electro-discharge-machined radial notch with roughened sides to radial pitch-catch normal mode and 60 degree shear mode transducers indicated considerable difficulty of detection (2), especially for radial pitch-catch. This difficulty is expected to be more severe in the case of tight fatigue cracks, i.e., cracks which may occur in the near-bore region in the presence of residual compressive stress resulting from creep or plastic relaxation.

ROTOR EXAMINATIONS

The Electric Energy Co. Joppa No. 3 IP and the Duke Power Co. Buck No. 6 IP-LP rotors were selected for detailed nondestructive and destructive examinations on the basis of reviews of inspection records, size of the forging, and year of installation. Both were reported by the manufacturer to be air melt Class C-1 Cr-Mo-V forgings and were retired by the utilities on the basis of the manufacturer's recommendations. Standard commercial practice was followed in the initial examinations. The detailed procedures and results are given in Ref. (2). Many small indications were found in both rotors, as illustrated in Fig. 3-1 for a 10-in.-long section of Joppa No. 3. This figure gives the probability density of indications as a function of equivalent flat-bottom hole area, determined from a calibration block containing the standard reflectors used to set the threshold detection levels of the two systems, and shows only the radial pitch-catch indications. These results have been corrected for the decrease in signal amplitude with metal path distance from the bore surface. Shear wave data was also obtained from both rotors with one of the commercial systems.

Obviously, the sensitivities of the two systems are very different. In addition, this variability has also been observed between reinspections using the same system, and accounts for a significant lack of reproducibility; however, it must be

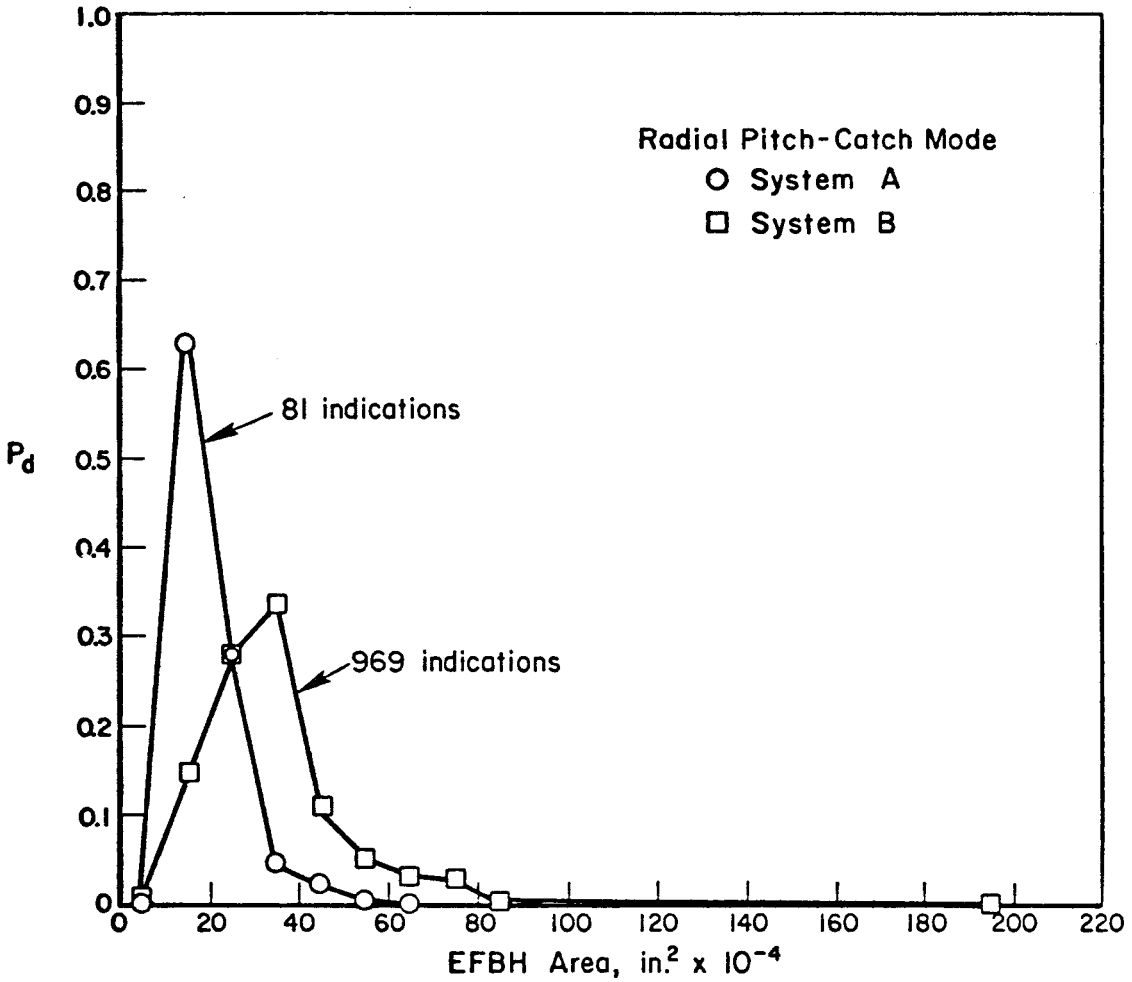

Figure 3-1. Distribution Of Amplitude Indications In Joppa No. 3

emphasized that the flaws in the Buck and Joppa rotors are small and relatively widely spaced, so that the system performance illustrated here should not necessarily be interpreted as a barrier to determining rotor integrity. In general, high resolution is required to evaluate the severity of closely-spaced defects within a cluster, and a high level of reproducibility is required to determine the generation or growth of flaws between successive examinations, which would indicate a potential fracture. From the Gallatin failure analysis, it appears that area fractions of small flaws on the order of 10 percent or less can initiate fracture; the volume fraction of flaws associated with this area fraction on the fracture surface may be appreciably less than 10 percent, as will be discussed in this section.

While linear elastic fracture mechanics predicts that high densities of clusters are required to initiate fracture from small defects, inelastic analysis indicates that the critical density of a cluster is relatively independent of individual defect size. Thus it is necessary to detect clusters of small defects and to estimate the density of the defects, while at the same time determining the radial-axial extent of the cluster. It should be reiterated here that the extent of the cluster must be of the order of the initial crack size that could grow to the critical size in order for the cluster to be of any structural consequence, regardless of the size or density of the constituent defects. Thus the nondestructive evaluation of a rotor like Joppa No. 3, containing a large number of small defects, consists of determining the most significant distribution of defects over an area equal to the initial crack size.

CLUSTER ANALYSIS

The evaluation of clustered defects requires the ability to discriminate between two or more small defects in close proximity. This discrimination involves the ultrasonic beam shape and width, the mechanical scan path of the transducer, and the detection threshold level. The broader the beam and the greater the pitch between successive scans relative to the defect size, the lower the threshold level required for detection and the greater the uncertainty of detection. These relationships are illustrated in Fig. 3-2. It is clear that when the beam width is large relative to the defect, the system is only capable of measuring the beam width, while in the case of a defect which is about equal in size to or greater than the beam width, the system can measure the sum of the defect dimension and the beam width. Except for ideal reflectors, such as flat-bottom holes, no correlation between amplitude of the received signal and defect size has been found; apparently, the variations of orientation, shape and physical nature of the defect/matrix interface prevent any general measure of defect size from signal amplitude. Several consequences of the relationships shown in Fig. 3-2 are readily apparent:

- The beam width must be smaller than the minimum dimension of the initial crack that could propagate to critical size (a function of distance from the bore, as shown in Fig. 2-7);
- The beam width should be on the order of the minimum flaw size that is desired to be detected;
- The pitch of the scan should not exceed the minimum beam width (near the bore surface);
- The threshold level should be sufficiently high to avoid recording spurious indications from small defects (below the size required to be detected) or resulting from side lobes in the beam energy profile.

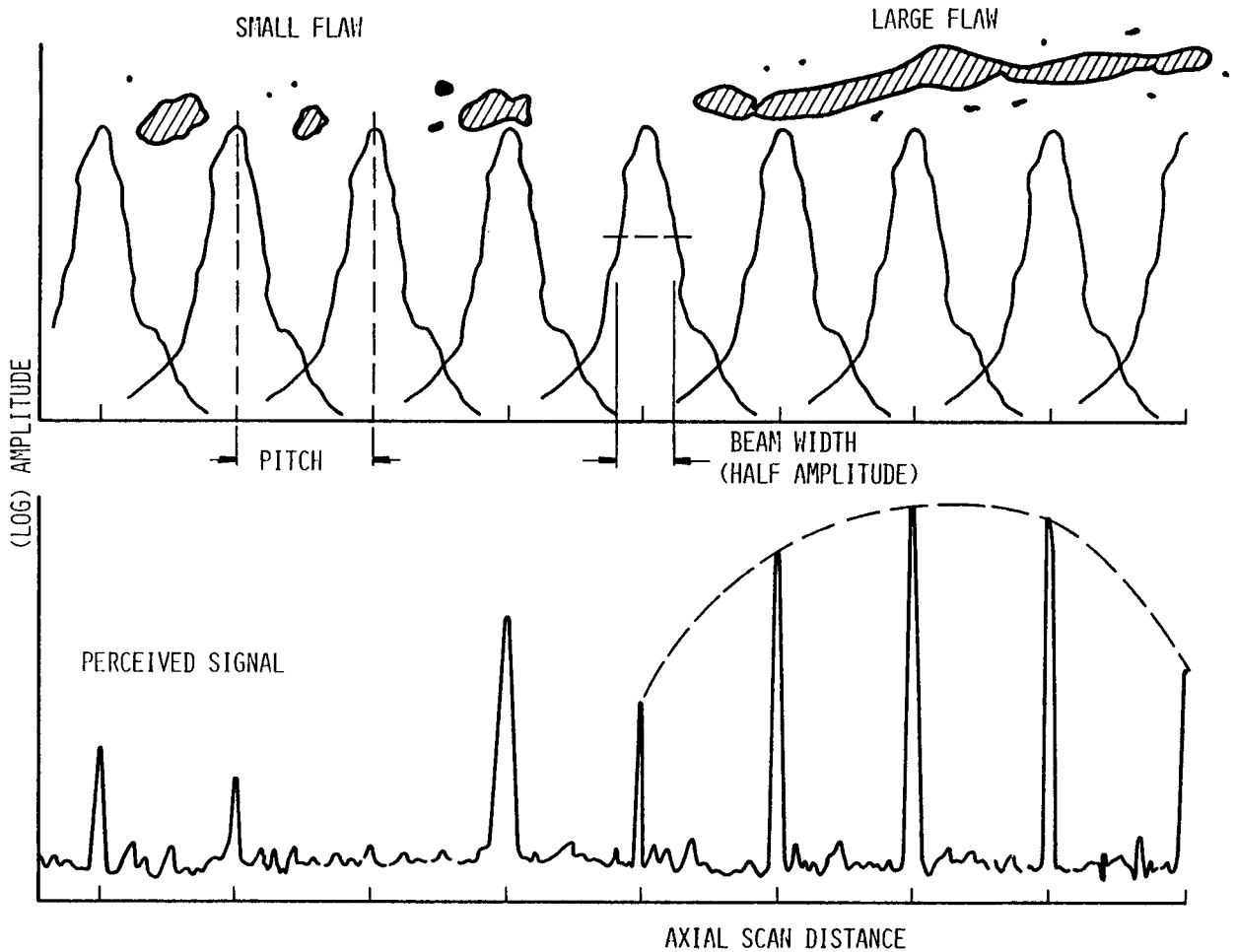

Figure 3-2. Relationship Between Flaw Size, Beam Width, Pitch, and Threshold

The flaws detected in the Buck and Joppa rotors have been generally much smaller than the beam width, and thus an attempt was made to establish a correlation between amplitude indications and physical sizes as revealed by metallographic sectioning. Average volume and area fractions were calculated for the highest density regions of the rotors. For this purpose the amplitude indication in terms of equivalent flat bottom hole area was arbitrarily taken to represent a spherical defect of radius equal to the EFBH radius. The volume fraction was then simply equal to the sum of the spherical volumes divided by the volume of the element. The metallographically-measured volume fraction was found by progressive sectioning. Figure 3-3 summarizes the results of this attempt at correlation from Ref. (2).

This type of correlation is considered inadequate to evaluate cluster severity and illustrates the need for improved ultrasonic procedures. Also, while no examples of cracking were found in any of the metallographic sections, it is felt that the commercial systems would have considerable difficulty discriminating between cracked and uncracked clusters. This important question remains to be resolved.

One further step is required to convert the volumetric flaw distributions to area distributions for fracture analysis. The most difficult aspect is the determination of the tangential distance over which defects can link up by crack growth or shear band rupture. This dimension is equivalent to the "roughness" of the radial-axial fracture surface, i.e., the out-of-plane deviations of the sub-critical crack growth. Clearly, the larger this distance relative to the defect size, the greater will be the area fraction of defects intersected by the fracture surface. For example, if a cluster consists of a uniform distribution of equiaxed defects which can interact over a distance s, the area fraction on the fracture surface is

$$A_F = \frac{3}{4} \frac{s}{r} V_F$$

where V_F is the volume fraction of flaws and r is the mean flaw radius.

The interaction distance s is a function of defect size, strain range, and flow stress; in addition, the plane strain conditions in the rotor increase the hydrostatic component of stress, which in turn tends to localize and concentrate shear

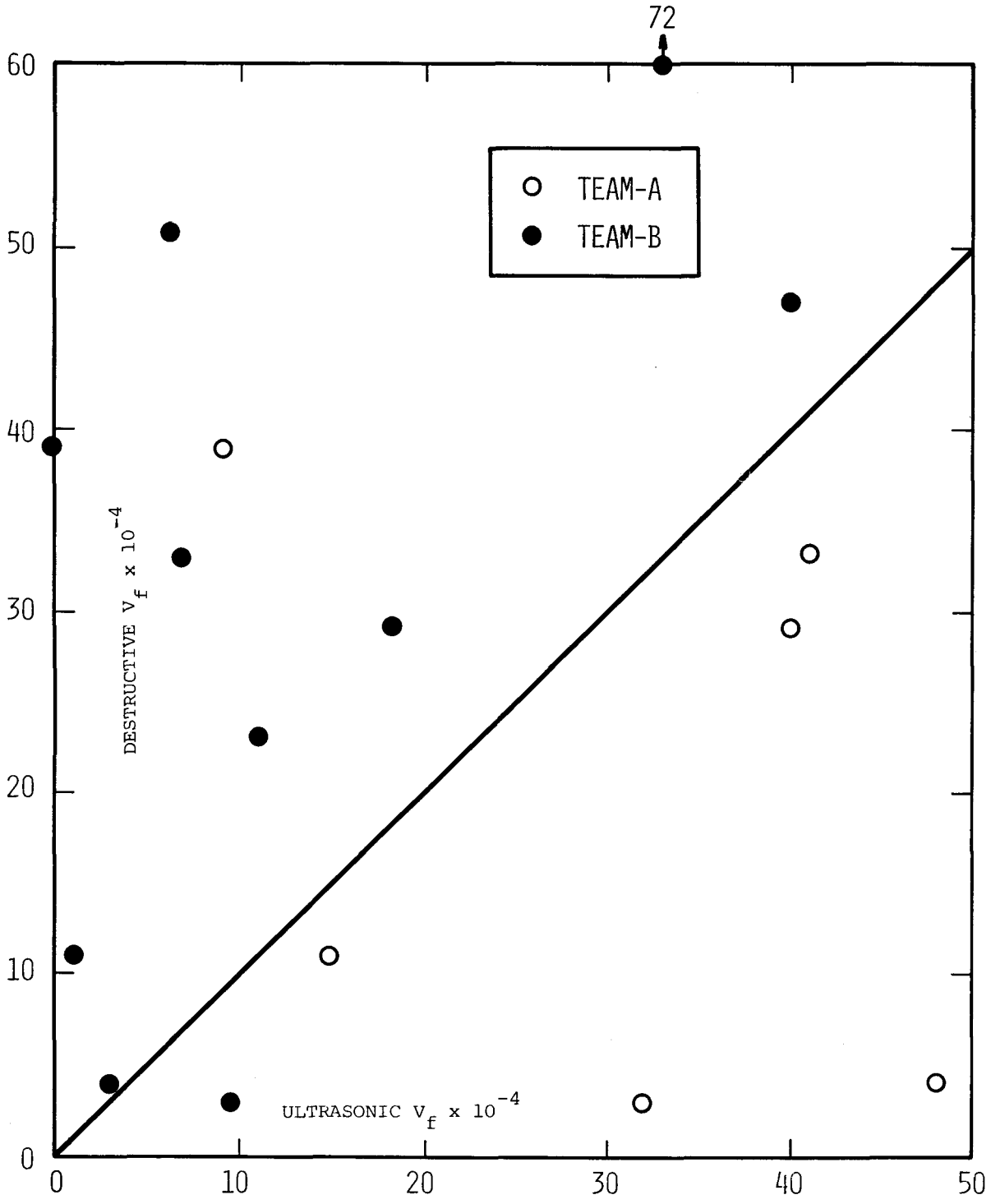

Figure 3-3. Correlation Between Indicated and Actual Flaw Volume Fractions

deformation between defects (Ref. 3). The prediction of this distance can be made by slip line field analysis or finite element modeling, as in Ref. (4). The value of s determined from a 3/4 in. length of the subcritical fracture surface of the Gallatin No. 2 IP rotor was about 0.005 inch.

REFERENCES

1. M. J. Golis and S. D. Brown, "Nondestructive Evaluation of Steam Turbine Rotors--An Analysis of the Systems and Techniques Utilized for In-Service Inspection", EPRI NP-744, April 1978.

2. Task 2 Final Report (in preparation).

3. S. I. Oh and S. Kobayashi, "Deformation Mode of Void-Growth and Coalescence in the Process of Ductile Fracture," AFML-TR-75-95, July 1975.

4. S. Nemat-Nasser, "Localization of Plastic Work in Two-Phase Alloys," Proceedings 14th Annual Meeting of the Society of Engineering Science, Nov. 1977, p. 757.

Section 4

MECHANICAL PROPERTY MEASUREMENT

Extensive mechanical property testing was carried out on the Gallatin and Joppa rotors to determine fracture toughness as a function of service exposure and test temperature, fatigue crack growth rates and the severity of defect distributions in low-cycle fatigue (LCF). Supplementary tests of the Gallatin material in creep-rupture and LCF were conducted to compare the base properties with results obtained on other 1 Cr-Mo-V forgings reported elsewhere. Creep-fatigue tests were run in the attempt to duplicate the intergranular subcritical crack growth mechanisms identified for the Gallatin rotor. The complete details of these tests are reported elsewhere (Ref. 1). The salient results and conclusions are as follows.

Gallatin Rotor Properties

Figures 4-1 and 4-2 summarize the LCF and stress-rupture properties, respectively, of the Gallatin material and compare them with results obtained for a vacuum-degassed 1 Cr-Mo-V rotor forging evaluated under a Metal Properties Council, Inc., program (Refs. 2, 3). The Gallatin LCF data is for 0.250 in. dia. axial strain-controlled specimens taken from both the near-bore origin area and from the periphery of the rotor. The near-bore specimens were found to contain bands of positive segregation similar to the Gallatin origin, along with small MnS inclusions. Fracture in all cases originated below the specimen surface at inclusions, but, apparently, the size of the inclusions was not sufficiently variable to induce scatter in the cyclic lifetime. Note in Figure 4-1 that a small, but significant, increase in LCF life is exhibited by the near-bore material. No reason for this difference has been verified, although it might be suggested that the presence of ferrite grains provides a mechanism for strain accommodation and crack retardation, as reported by researchers in England for creep crack growth in 1/2 Cr-Mo-V forgings (see discussion in Section 5). Some of the tests, as indicated, were held at the tensile strain limit for several hours in each cycle to introduce creep damage. While small reductions in cyclic life were obtained, the results do not differ significantly with hold times up to 24 hours. Of all the tests performed on Gallatin material, only the 24 hr. hold time LCF specimen (and a similar interrupted test) exhibited any intergranular fracture (similar to the failure origin

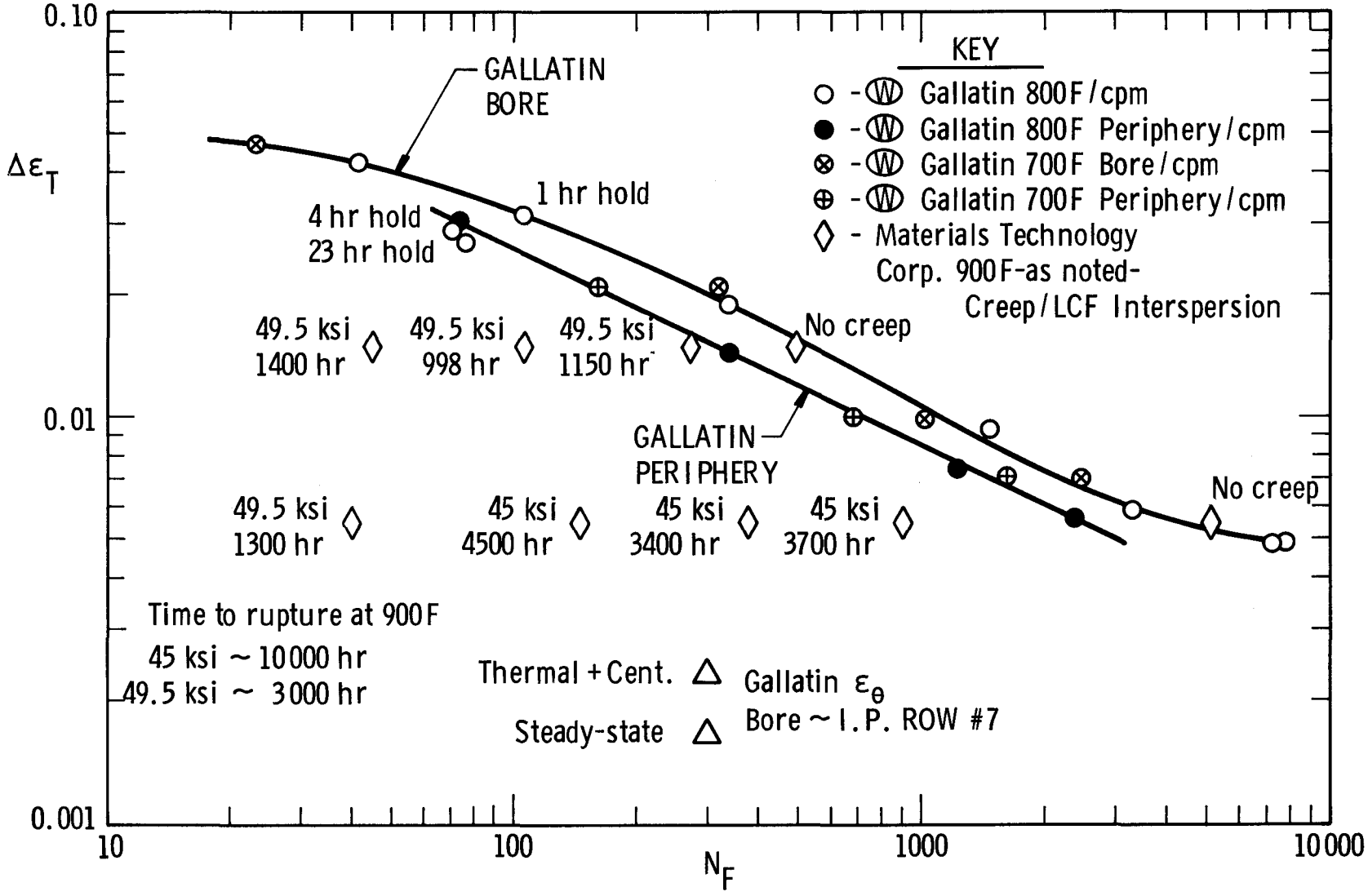

Figure 4-1. Low-Cycle Fatigue Data For 1 Cr-Mo-V Gallatin Material

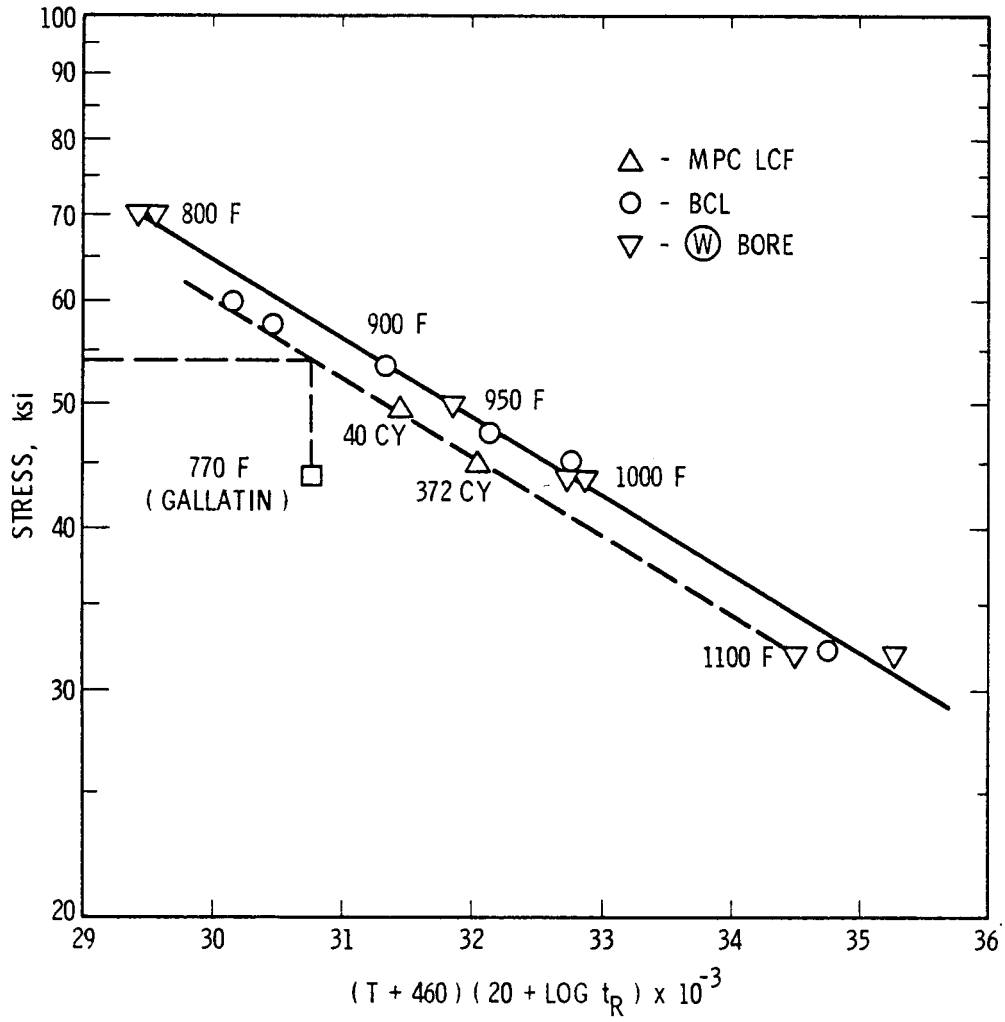

Figure 4-2. Larson-Miller Representation Of 1 Cr-Mo-V Stress-Rupture Data

of the rotor), although some intergranularity was reported in a low-temperature fracture in the Auger spectrometer in the course of measuring the concentration of trace elements (Ref. 1).

Also plotted in Figure 4-1 are the results of the creep-LCF interspersion tests conducted by Materials Testing Corp. for the Metal Properties Council. These tests combine axial strain cycles with periods of constant load, thus producing easily separable combinations of nominal LCF and stress-rupture damage (Ref. 3). In the limit, of course, these tests can be made to produce failure in stress-rupture in only one cycle. However, the significance of Figure 4-1 is that a large component of stress rupture in each cycle is required to explain the initiation of fracture in the Gallatin rotor in the absence of macroscopic defects.

The stress-rupture properties of near-bore Gallatin material are compared with the Metal Properties Council data in Figure 4-2 on the basis of the Larson-Miller parameter. The degree of scatter is small and the values are in agreement with other published data from similar forgings (Ref. 4). The interspersion test results show about a three-fold reduction in rupture lifetime relative to conventional test data; however, the base material data still does not predict the Gallatin fracture under the steady-state stress, time and temperature conditions at the origin.

Certain of the interspersion specimens were provided by the Metal Properties Council for metallographic evaluation. No evidence of intergranular cracking could be found, nor, in fact, was there any evidence of intergranular cavitation by transmission electron microscopy. While the Gallatin subcritical crack was intergranular, no evidence of intergranular cavitation could be found adjacent to the fracture surface. Therefore, some of the discrepancy between the stress-rupture data and the Gallatin failure point may be attributed to this difference in crack growth mechanism. A substantial portion of the difference may result from the presence of a relatively high area fraction of MnS inclusions distributed in clusters along the subcritical crack. Although creep crack growth rate data at the origin temperature is not available, the presence of inclusions may be assumed to increase the local stress in the ligaments, in this case by about the 8 percent reported as the maximum observed area fraction. This raises the local stress to around 48 ksi, or 5 ksi lower than would be required to predict rupture from the interspersion test data in Figure 4-2.

Fracture Toughness

Values of K_{IC} and J_{IC} from both Gallatin and Joppa are summarized in Figure 4-3. Good agreement between fracture toughness and FATT according to the Begley-Logsdon correlation (Ref. 1) was reported. No evidence of temper embrittlement was found in these rotors, nor was there appreciable difference between hot and cold sections of the rotors.

In contrast, severe embrittlement has been identified near the reheat stage of the Buck rotor with a FATT in the vicinity of 575°F and reduced values of impact energy at room temperature and the upper shelf. No fracture mechanics data is yet available. Fracture surfaces show a mixture of intergranularity and ductile rupture. The coarse prior austenite grain size (ASTM 4 to 0) indicates a high austenitizing temperature which, together with verified high levels of trace elements such as phosphorous and tin, would make the forging susceptible to temper embrittlement during long exposure times to reheat steam temperature. Measurements of FATT and fracture toughness at several axial sections of the Buck rotor are underway, as are austenite grain size measurements on other Class C rotors.

Figure 4-3 also shows the toughness data which is incorporated into STRAP's Fracture Analysis Code. The curve is conservative for unembrittled material over the entire temperature range, but it is not conservative for temper-embrittled material such as exists near the inlet stage of the Buck rotor.

Fatigue Crack Growth Tests

A series of compact-tension fatigue crack growth rate tests was conducted on Gallatin and Joppa material with various hold times and frequencies at several temperatures. It was hoped that the data could be represented by a single parameter and would represent the significant effects of time and temperature. However, the data failed to conform to parametric generalization.

In tests on the Joppa material, it was possible to reduce the data to the form

$$\frac{da}{dN} = C\ (\nu,\ T)\ \Delta K^{2.7}$$

over the frequency range

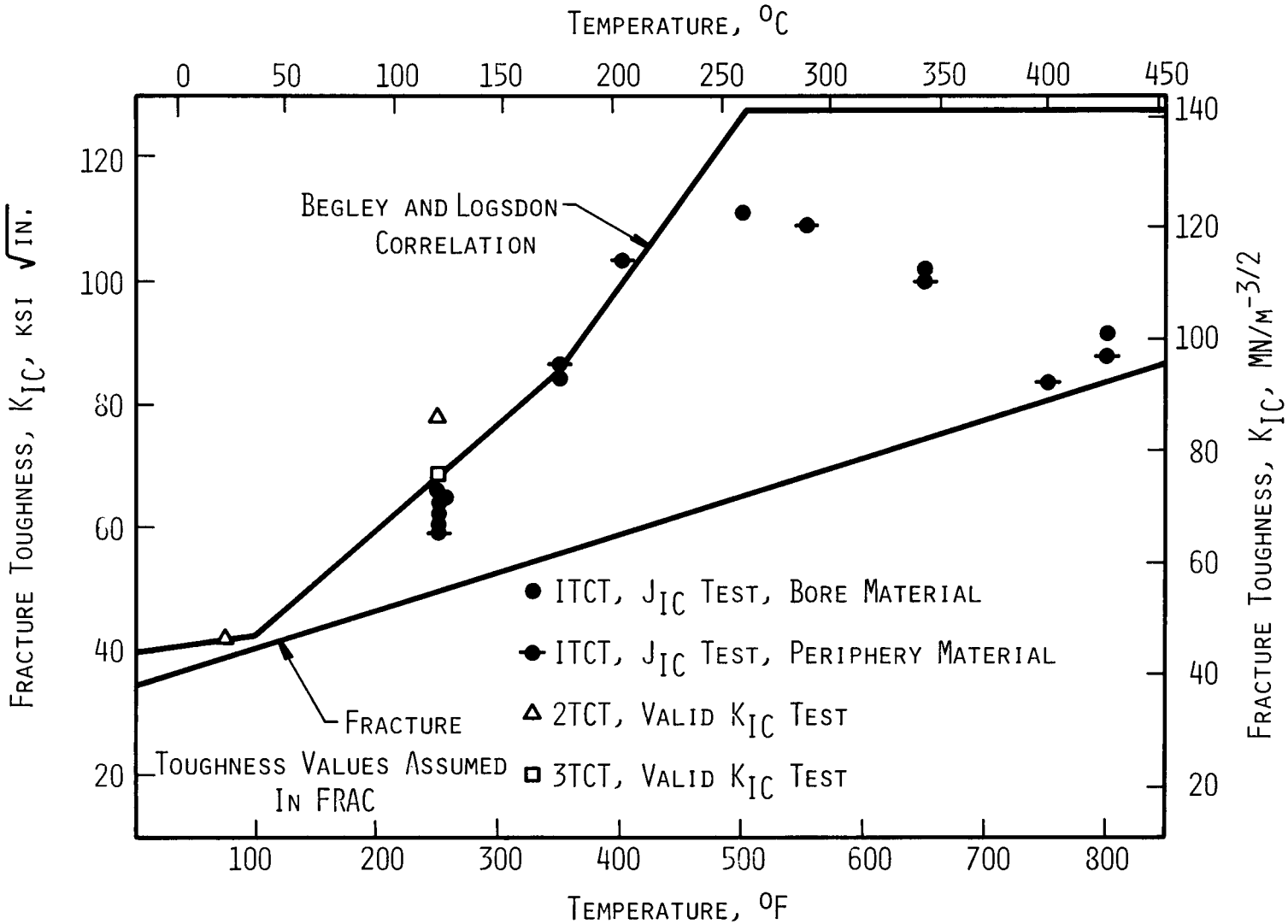

Figure 4-6. Fracture Toughness Data

$$0.0017 \text{ Hz} \leq \nu \leq 1.0 \text{ Hz}$$

The coefficient $C(\nu, T)$ is plotted in Figure 4-4 as a function of $1/\nu$ using temperature as a parameter.

The results of the 800°F, 1 Hz tests on Gallatin material also fit this crack growth relation quite well. It was hoped, therefore, that the results of hold time tests on the Gallatin material would be obtainable from an extrapolation of the Joppa data. Two hold time tests were run at 800°F using Gallatin material; the growth rates from these tests were given by

$$\text{15 minute hold} - \frac{da}{dN} = 2.6 \times 10^{-12} \Delta K^{4.54}$$

$$\text{24 hour hold} - \frac{da}{dN} = 1.3 \times 10^{-11} \Delta K^{4.54}$$

Thus, the hold time results had a steeper slope and smaller coefficients than did the tests which did not include a hold time. This means that the growth rates for the hold time test will be faster only at high ΔK values. Comparing the 1 Hz and the 15 minute hold time Gallatin tests, the growth rates are higher for the 1 Hz test until ΔK exceeds 40 ksi $\sqrt{\text{in}}$. The 24 hour hold time growth rate is about three times faster than the 15 minute hold time rate so the crossover point between the hold time and the steady sinusoidal rate occurs earlier, at about 15 ksi $\sqrt{\text{in}}$.

From Figure 4-4, the extrapolated values of the coefficients for the hold time frequency are:

$$C(1/\nu = 900, 800^{\circ}\text{F}) = 2.7 \times 10^{-9}$$

$$C(1/\nu = 8.6 \times 10^{4}, 800^{\circ}\text{F}) = 6.8 \times 10^{-9}$$

Comparing the results at several levels of stress intensity, the growth rates, da/dN (in./cycles) are:

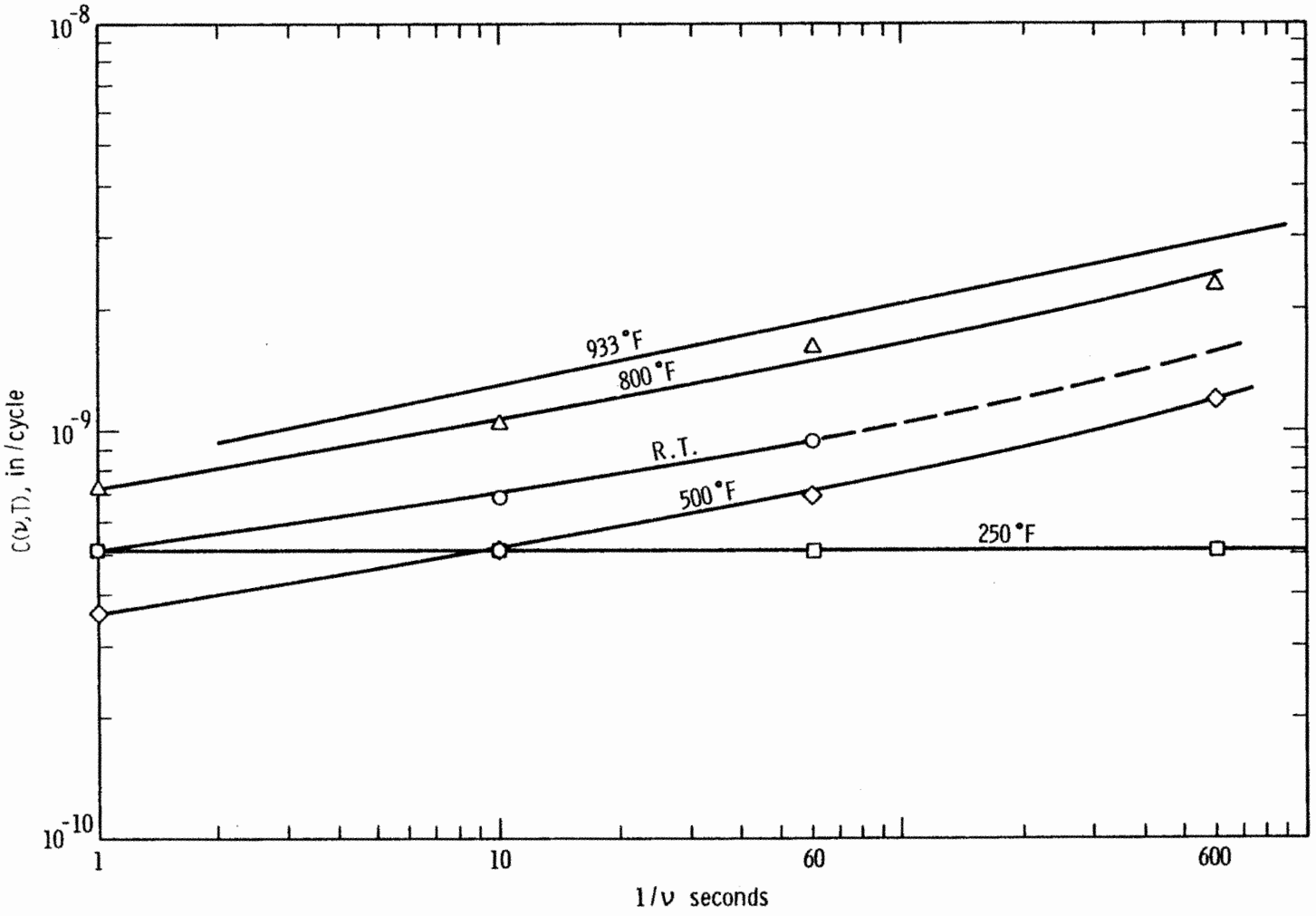

Figure 4-4. Fatigue Crack Growth Coefficient Data

	HOLD TIME		EXTRAPOLATED SINUSOIDAL	
ΔK, ksi$\sqrt{in}$.	15 min	24 hr	$1/\nu$ = 900 sec	8.6 x 10^4sec
10	9.0×10^{-8}	4.5×10^{-7}	1.4×10^{-6}	3.4×10^{-6}
25	5.8×10^{-6}	2.9×10^{-5}	1.6×10^{-5}	4.0×10^{-5}
40	4.9×10^{-5}	2.4×10^{-4}	5.7×10^{-5}	1.4×10^{-4}
55	2.1×10^{-4}	1.0×10^{-3}	1.4×10^{-4}	3.4×10^{-4}

These comparisons indicate that at low ΔK values, the hold time growth rates are much slower. Since the bulk of structural life is spent growing small cracks, this comparison indicates that the hold time data would predict longer lives than the continuous cycling data.

REFERENCES

1. G. A. Clarke, T. T. Shih, and L. D. Kramer, Final Report Research Project: EPRI RP502, Task IV, Mechanical Properties Testing, Reliability of Steam Turbine Rotors, March 1978.

2. C. E. Jaske and H. Mindlin, "Elevated Temperature Low-Cycle Fatigue Behavior of 2 1/4 Cr-1 Mo-1/4 V Steels," Symposium on 2 1/4 Chrome 1 Molybdenum Steel in Pressure Vessels and Piping, Metal Properties Council, Second Annual Pressure Vessels and Piping Conference, Denver, Sept. 1970, ASME Publication G11, 1971, pp. 137-210.

3. R. M. Curran and B. M. Wundt, "Continuation of a Study of Low-Cycle Fatigue and Creep Interaction in Steels at Elevated Temperatures," 1976 ASME-MPC Symposium on Creep-Fatigue Interaction, ASME Publication G113, 1976, pp. 203-282.

4. R. M. Goldhoff and H. J. Beattie, Jr., "The Correlation of High-Temperature Properties and Structures in 1 Cr-Mo-V Forging Steels," Transactions of the Metallurgical Society of AIME, 233, 1965, pp. 1743 - 1756.

Section 5

DISCUSSION OF GALLATIN ROTOR BURST

Throughout the RP502 project there has been a continuing review and discussion of the mechanism of the subcritical crack growth in the Gallatin No. 2 IP rotor with particular interest in the possibility of a unique microstructure feature that would raise questions of material variability, viz., the origin, detection and statistical frequency of occurrence of such microstructure. On the other hand, there remains the possibility that the mechanical property testing to date has not been adequate to characterize the rate of subcritical crack growth. In this regard, it should be reiterated that the only intergranular fracture surface reproduced in laboratory tests of material from the Gallatin rotor was a 24 hr. hold time, low-cycle fatigue test conducted at about ten times the total strain range calculated for the origin area. The manufacturer's failure analysis pointed to an increased amount of fine-grained ferrite in the banded regions of the fracture origin area relative to other regions of the Gallatin rotor; the carbide distribution in these grain boundaries, consisting of coarse $M_{23}C_6$, and the depletion of fine V_4C_3 particles in the adjacent matrix, suggested the possibility of a reduced resistance to intergranular crack growth either during the cold start transient or under prolonged steady-state operation at elevated temperature.

Independent transmission electron microscopy and optical metallographic examination of specimens from the Gallatin subcritical crack region as well as material from a different vacuum-degassed 1 Cr-Mo-V rotor under study by the Metal Properties Council (1) was carried out in order to determine the extent of the microstructural differences between the two rotors. The project participants agreed to the following general conclusion after extensive review and discussion: "The Gallatin rotor microstructure is similar in nature to the microstructure of the other rotor material examined. However, the extent of these potentially deleterious microstructural features is more pronounced in the (banded) Gallatin material. None of the Gallatin specimen tests run to date have yielded results which can be said to explain unequivocally the Gallatin failure mechanism."

The detailed conclusions are summarized in Appendix A.

An intensive effort to characterize creep crack growth in 1/2 Cr-Mo-V is underway at the Central Electricity Research Laboratories in England. While the composition differs from the forgings under consideration in RP502, the detailed microstructural features, including grain boundary carbide morphology, are similar. Testing has been reported exclusively at 565 C (1050 F), well above the Gallatin origin temperature. However, the significant conclusion reached by Gooch et. al. (2) is that "...The effect of small amounts of ferrite along prior austenite grain boundaries in an otherwise baintic structure is to facilitate strain accommodation, thus inhibiting grain boundary cavity nucleation." Constant-load creep crack growth rate tests showed that increasing amounts of ferrite significantly reduced the crack growth rate relative to 100% bainite. On the other hand, these authors found that varying the amount of trace elements (arsenic, tin, antimony and phosphorus) changed the creep crack growth rate by two orders of magnitude both for tempered and untempered 1/2 Cr-Mo-V.

It is not possible at the present time to predict creep crack growth rates at the Gallatin origin temperature or to evaluate the effects of intermittant strain cycling or plane strain conditions that exist within the body of the rotor. Notwithstanding these uncertainties, it appears that the possibility of predicting the lifetime of Gallatin from creep crack growth data is more promising than is an appeal to differences in microstructure that have not proved deleterious in any mechanical test performed to date. Given the proximity of Gallatin to stress-rupture failure under the net ligament stress (Figure 4-2) and the possible errors in the heat transfer analysis, it is natural to regard the material variability for the moment as a second-order effect until the mechanical property data has been generated and the temperature distribution verified.

REFERENCES

1. R. M. Curran and B. M. Wundt, "Continuation of a Study of Low-Cycle Fatigue and Creep Interaction in Steels of Elevated Temperatures," 1976 ASME-MPC Symposium on Creep-Fatigue Interaction, ASME, New York, G00112, p. 203.

2. D. J. Gooch, J. R. Haigh and B. L. King, "Relationship Between Engineering and Metallurgical Factors in Creep Crack Growth," Metal Science, 11, 11, Nov. 1977, pp. 545-550.

APPENDIX A

Conclusions of RP502 Participants from the Evaluation of the TVA Gallatin No. 2 IP Rotor Microstructure.

1. Intergranular cracking occurs on high angle boundaries, regardless of grain size, in the range from 10 to 50 microns.

2. Sub-boundaries, on the order of one micron, appear to play no role in the cracking process.

3. Intergranular cracking occurs in bands of positive dendritic segregation.

4. There are more fine-grained areas in the banded regions than in the matrix.

5. There are more fine-grained areas in the banded regions of the Gallatin rotor than in the specimens from the Metal Properties Council creep-fatigue interspersion tests.

6. The volume fraction of MnS inclusions in the Gallatin rotor is larger than in the Buck or Joppa rotors.

7. The reported area fraction of MnS inclusions on the fracture origin surface of the Gallatin rotor (7 to 8%) is higher than the average matrix area fraction determined from metallographic sectioning.

8. The Gallatin fracture origin contains no silicates or oxides, in contrast to the Joppa and Buck rotors.

9. There is more proeutectoid ferrite visible by TEM in the Gallatin rotor than in the MPC specimens.

10. Areas denuded of V_4C_3 exist in the ferrite along the grain boundaries.

11. The Gallatin origin has more coarse, semi-continuous $M_{23}C_6$ carbides than are apparent in unbanded regions of the rotor, but is similar to the MPC specimens in this respect. The large $M_{23}C_6$ carbides are associated with carbide-denuded zones.

12. No evidence of concentrated strain is observed in carbide-denuded zones.

13. No grain goundary cavitation is observed by TEM or optical microscopy.

In addition to these conclusions, the following comments were offered by the participants:

- The composition-temperature diagram for the reported local chemistry would suggest that less ferrite should be seen in the banded regions, in contrast with metallographic observations.

- Ferrite is more liable to be found in the slower-cooled regions.

- It is generally observed that the bainite in rotor steel contains some denuded zones.

- The reported level of phosphorus and tin at the Gallatin origin, when compared with literature data, implies an (adverse) influence on creep strength.

- None of the mechanical tests performed to date on near-origin specimens from the Gallatin rotor shows any significant decrease in mechanical properties compared to similar data on specimens from other areas.